In general, ERK and JNK kinases phosphorylate ternary complex factors (TCF), which cooperate with serum response factor (SRF) to induce *EGR1* transcription in vascular biology (22). *EGR1* can displace Sp1 and other transcription factors, and EGR1 transactivation leads to the transcription of many EGR1-target genes. To date, several putative EGR1-target genes related to cancer have been identified, including cyclin D, EGFR, FGF, IGF-I, thymidine kinase, PDGF-A, Bcl2, CD44, p53, PTEN, TNF-α and VEGF. Further investigation of the biological role of EGR1 overexpression in mutant *EGFR* may lead to a better understanding of the roles of mutant *EGFR* in cancer cells.

In conclusion, it was found that mutant *EGFR* induced EGR1 overexpression and that this overexpression was correlated with EGFR signal activation through ERK1/2. These results provide a novel insight into the oncogenic properties of EGFR in cancer cells.

Acknowledgements

This work was supported by funds for the Third-Term Comprehensive 10-Year Strategy for Cancer Control and the program for the promotion of Fundamental Studies in Health Sciences of the National Institute of Biomedical Innovation (NiBio) and the Japan Health Sciences Foundation.

We thank Dr. Richard Simon and Dr. Amy Peng for providing the BRB ArrayTools software.

References

1 Cowley GP, Smith JA and Gusterson BA: Increased EGF receptors on human squamous carcinoma cell lines. Br J Cancer *53*: 223-229, 1986.

2 Gusterson B, Cowley G, McIlhinney J, Ozanne B, Fisher C and Reeves B: Evidence for increased epidermal growth factor receptors in human sarcomas. Int J Cancer *36*: 689-693, 1985.

3 Karamouzis MV, Grandis JR and Argiris A: Therapies directed against epidermal growth factor receptor in aerodigestive carcinomas. JAMA *298*: 70-82, 2007.

4 Rocha-Lima CM, Soares HP, Raez LE and Singal R: EGFR targeting of solid tumors. Cancer Control *14*: 295-304, 2007.

5 Mitsudomi T, Kosaka T, Endoh H *et al*: Mutations of the epidermal growth factor receptor gene predict prolonged survival after gefitinib treatment in patients with non-small-cell lung cancer with postoperative recurrence. J Clin Oncol *23*: 2513-2520, 2005.

6 Paez JG, Janne PA, Lee JC *et al*: EGFR mutations in lung cancer: correlation with clinical response to gefitinib therapy. Science *304*: 1497-1500, 2004.

7 Pao W, Miller V, Zakowski M *et al*: EGF receptor gene mutations are common in lung cancers from "never smokers" and are associated with sensitivity of tumors to gefitinib and erlotinib. Proc Natl Acad Sci USA *101*: 13306-13311, 2004.

8 Tokumo M, Toyooka S, Kiura K *et al*: The relationship between epidermal growth factor receptor mutations and clinicopathologic features in non-small cell lung cancers. Clin Cancer Res *11*: 1167-1173, 2005.

9 Amann J, Kalyankrishna S, Massion PP *et al*: Aberrant epidermal growth factor receptor signaling and enhanced sensitivity to EGFR inhibitors in lung cancer. Cancer Res *65*: 226-235, 2005.

10 Arao T, Fukumoto H, Takeda M, Tamura T, Saijo N and Nishio K: Small in-frame deletion in the epidermal growth factor receptor as a target for ZD6474. Cancer Res *64*: 9101-9104, 2004.

11 Koizumi F, Shimoyama T, Taguchi F, Saijo N and Nishio K: Establishment of a human non-small cell lung cancer cell line resistant to gefitinib. Int J Cancer *116*: 36-44, 2005.

12 Sakai K, Arao T, Shimoyama T *et al*: Dimerization and the signal transduction pathway of a small in-frame deletion in the epidermal growth factor receptor. FASEB J *20*: 311-313, 2006.

13 Sakai K, Yokote H, Murakami-Murofushi K, Tamura T, Saijo N and Nishio K: In-frame deletion in the EGF receptor alters kinase inhibition by gefitinib. Biochem J *397*: 537-543, 2006.

14 Matsumoto K, Yokote H, Arao T *et al*: N-Glycan fucosylation of epidermal growth factor receptor modulates receptor activity and sensitivity to epidermal growth factor receptor tyrosine kinase inhibitor. Cancer Sci *99*: 1611-1617, 2008.

15 Igarashi T, Izumi H, Uchiumi T *et al*: Clock and ATF4 transcription system regulates drug resistance in human cancer cell lines. Oncogene *26*: 4749-4760, 2007.

16 Lo LW, Cheng JJ, Chiu JJ, Wung BS, Liu YC and Wang DL: Endothelial exposure to hypoxia induces Egr-1 expression involving PKCalpha-mediated Ras/Raf-1/ERK1/2 pathway. J Cell Physiol *188*: 304-312, 2001.

17 Adamson ED and Mercola D: Egr1 transcription factor: multiple roles in prostate tumor cell growth and survival. Tumour Biol *23*: 93-102, 2002.

18 Baron V, Adamson ED, Calogero A, Ragona G and Mercola D: The transcription factor Egr1 is a direct regulator of multiple tumor suppressors including TGFbeta1, PTEN, p53, and fibronectin. Cancer Gene Ther *13*: 115-124, 2006.

19 Adamson E, de Belle I, Mittal S *et al*: Egr1 signaling in prostate cancer. Cancer Biol Ther *2*: 617-622, 2003.

20 Lynch TJ, Bell DW, Sordella R *et al*: Activating mutations in the epidermal growth factor receptor underlying responsiveness of non-small-cell lung cancer to gefitinib. N Engl J Med *350*: 2129-2139, 2004.

21 Ferraro B, Bepler G, Sharma S, Cantor A and Haura EB: EGR1 predicts PTEN and survival in patients with non-small-cell lung cancer. J Clin Oncol *23*: 1921-1926, 2005.

22 Silverman ES and Collins T: Pathways of Egr-1-mediated gene transcription in vascular biology. Am J Pathol *154*: 665-670, 1999.

Received October 20, 2008
Revised January 19, 2009
Accepted February 13, 2009

research articles Journal of proteome research

Identification of Predictive Biomarkers for Response to Trastuzumab Using Plasma FUCA Activity and N-Glycan Identified by MALDI-TOF-MS

Kazuko Matsumoto,[†,§,#] Chikako Shimizu,[‡,#] Tokuzo Arao,[†] Masashi Andoh,[‡] Noriyuki Katsumata,[‡] Tsutomu Kohno,[‡] Kan Yonemori,[‡] Fumiaki Koizumi,[∥] Hideyuki Yokote,[†] Kenjiro Aogi,[⊥] Kenji Tamura,[‡] Kazuto Nishio,[*,†] and Yasuhiro Fujiwara[‡]

Department of Genome Biology, Kinki University School of Medicine, Osaka, Japan, Medical Oncology, National Cancer Center Hospital, Tokyo, Japan, First Department of Internal Medicine, Osaka Medical College, Osaka, Japan, Shien Lab, National Cancer Center Hospital, Tokyo, Japan, and Department of Surgery, National Hospital Organization Shikoku Cancer Center, Matsuyama, Japan

Received August 19, 2008

The aim of this study was to identify glycobiological biomarkers that indicate sensitivity to trastuzumab, a humanized monoclonal antibody against HER2 in plasma samples from breast cancer patients. Plasma samples were obtained from 24 breast cancer patients treated with trastuzumab monotherapy. The catalytic activities of plasma α1-6, fucosyltransferase (FUT8) and α-L fucosidase (FUCA) were analyzed using high-performance liquid chromatography (HPLC) and spectrophotometer, respectively. The plasma N-glycan profiles were investigated using matrix-assisted laser desorption/ionization time-of-flight mass spectrometry (MALDI-TOF-MS). Plasma FUT8 activity was not significantly correlated with either the clinical response or progression-free survival (PFS). On the other hand, plasma FUCA activity was significantly correlated with PFS ($p < 0.05$). The MALDI-TOF-MS analysis of the plasma N-glycan profile revealed that the expression of 2534 *m/z* N-glycan was lower in patients with progressive disease (PD) and was correlated with PFS. Low expression of 2534 *m/z* N-glycan discriminated between PD and non-PD with 75% sensitivity and 82% specificity. We demonstrated that the plasma FUCA activity and 2534 *m/z* N-glycan may be predictive biomarkers of sensitivity to trastuzumab. Our results suggest that glycosylation analysis may provide useful information for determining clinical cancer therapy and provide novel insight into biomarker studies using glycobiological tools in the field of breast cancer.

Keywords: FUT8 • FUCA • N-glycan • trastuzumab • breast cancer

Introduction

The glycosylation of proteins is an important post-translational modification that plays a critical role in cancer biology including cellular growth, differentiation, adhesion and metastasis.[1−4] Specific carbohydrate chains and glycosyltransferase are associated with the biological functions of cancer cells.[5,6] Recently, many researchers have evaluated the use of glycosylated proteins, such as carbohydrate antigens CA19−9 and CA125, as biomarkers for early diagnosis or tumor progression.[7−9]

The fucosylation of N-linked oligosaccharides is one of the most important glycosylation events in biological function, including cancer.[10,11] For example, fucosylated α-fetoprotein is a highly specific tumor marker of hepatocellular carcinoma.[12] α1-6, Fucosyltransferase (FUT8) is known to transfer a fucose residue to N-linked oligosaccharides on glycoproteins.[13] A series of studies have demonstrated that nonfucosylated antibody, which is produced by the knockout of the FUT8 gene, enhances antibody-dependent cellular cytotoxicity (ADCC) and the cytotoxic effect of the antibody.[14−16] These results indicate that FUT8 plays an important role in ADCC activity. α-L fucosidase (FUCA), on the other hand, is a lysosomal hydrolase that has been identified in tissues and serum. Serum FUCA activity is reportedly correlated with early detection in hepatocellular carcinoma[17] and may be a useful prognostic marker and a predictive marker of tumor recurrence in colorectal cancer.[18,19]

HER2 (also known as NEU, EGFR2, or ERBB2) is a member of the epidermal growth factor receptor (EGFR) family. HER2 is amplified in 25−30% of human primary breast cancers and predicts a poor prognosis.[20−22] Trastuzumab (Herceptin; Roche, Basel, Switzerland), a humanized monoclonal antibody against HER2, is a potent anticancer agent that is used in standard chemotherapy against HER2-overexpressing breast cancer in

* To whom correspondence should be addressed. Kazuto Nishio, Department of Genome Biology, Kinki University School of Medicine, 377-2 Ohno-Higashi, Osaka-Sayama, Osaka, Japan. Tel: +81-72-366-0221. Fax: +81-72-366-0206. E-mail: knishio@med.kindai.ac.jp.
† Kinki University School of Medicine.
§ Osaka Medical College.
‡ Medical Oncology, National Cancer Center Hospital.
# These authors contributed equally to this work.
∥ Shien Lab, National Cancer Center Hospital.
⊥ National Hospital Organization Shikoku Cancer Center.

10.1021/pr800655p CCC: $40.75

Published on Web 01/13/2009

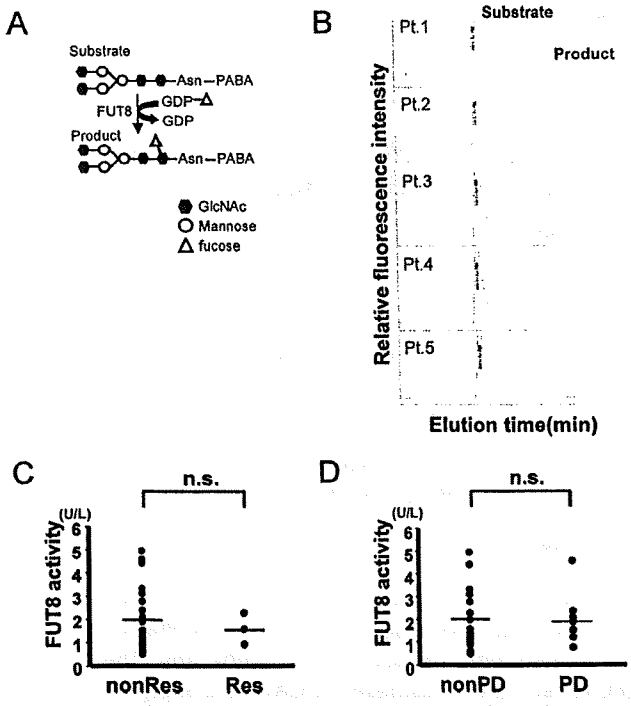

Figure 1. (A) Schema of α1-6, fucosyltransferase (FUT8) reaction used to measure FUT8 enzymatic activity. Asn, asparagine; PABA, 4-(2-pyridylamino) butylamine. (B) HPLC data for plasma FUT8 activities in clinical samples. The substrate (GnGn-bi-Asn-PABA) is fucosylated by FUT8 and detected as the product. FUT8 activity is measured using HPLC. The enzyme activities were analyzed in duplicate. (C) Plasma FUT8 activity and clinical response. Res, responder group (complete response + partial response); non-Res, nonresponder group (stable disease + progressive disease). n.s.: not significant. (D) Plasma FUT8 activity and clinical response. PD, progressive disease group; nonPD, nonprogressive disease group. n.s.: not significant.

combination with other chemotherapeutic agents.[23,24] In some patients with HER2 overexpression, however, trastuzumab dose not have any anticancer effect. In addition, trastuzumab can induce severe adverse effects, such as cardiac dysfunction.

Therefore, biomarkers are needed to predict the clinical outcome of trastuzumab therapy in patients with breast cancer. We previously reported that trastuzumab-induced ADCC is a major mechanism of action,[25] in addition to the effects of anti-EGFR antibody.[26] We have also identified a sensitivity determinant factor for EGFR-targeting drugs[27,28] and recently demonstrated that FUT8 regulated the fucosylation level of EGFR and modifies EGF-mediated cellular growth and sensitivity to EGFR tyrosine kinase inhibitor.[29]

In the present study, we attempted to identify predictive biomarkers of sensitivity to trastuzumab, focusing on fucosylation and glycosylation. For this purpose, plasma FUT8 and FUCA activity and the N-glycan profiles were examined in breast cancer patients treated with trastuzumab monotherapy.

Materials and Methods

Patients and Blood Samples. This prospective study was started in August 2005 and enrollment at the National Cancer Center Hospital and Shikoku Cancer Center Hospital was completed in August 2007. Eligible patients had histologically confirmed, nonlife-threatinig, postoperative recurrent or stage IV HER2-positive breast cancer, and were intended to receive trastuzumab monotherapy. The HER2 status was confirmed using immunohistochemistry (IHC) 3+ or fluorescence in situ hybridization (FISH)-positive utilizing core needle biopsy (CNB) samples of the tumor tissue. All the patients were treated with trastuzumab (4 mg/kg on day 1 and thereafter at a dose of 2 mg/kg weekly), and 24 patients were evaluated. The response to trastuzumab therapy was evaluated based on a CT scan, magnetic resonance imaging (MRI) or ultrasound examination of the tumor before and 8 weeks after treatment and was classified according to the Response Evaluation Criteria in Solid Tumors. Plasma samples were obtained immediately before trastuzumab treatment, centrifuged and stored at −80 °C. The study was approved by the Institutional Review Boards of the National Cancer Center Hospital, Kinki University Hospital and Shikoku Cancer Center Hospital, and written informed consent was obtained from all the patients.

Table 1. Clinical Characteristics of Study Population[a]

characteristics		no. of patients	%
Age	Mean	60	
	Range	28−76	
Prior chemotherapy	Present	17	71
	Absent	6	25
	ND	1	4
Prior radiotherapy	Present	14	58
	Absent	9	38
	ND	1	4
PS	0	8	33
	1	15	63
	2	1	4
Metastasis	Lung	15	63
	Liver	3	13
	Bone	5	21
	Brain	2	8
	LN	10	42
	Others	2	8
Hormone receptor	ER (+)	12	50
	ER (−)	12	50
	PgR (+)	11	46
	PgR (−)	12	50
	ND	1	4

[a] ND, not determined; PS, performance status; ER, estrogen receptor; PgR, progesterone receptor.

FUT8 Activity Assay. The method used to perform the FUT8 activity assay has been previously described.[30] Briefly, the fluorescent substrate (GnGn-bi-Asn-PABA, Figure 1A) was purchased from Peptide Institute, Inc. (Osaka, Japan). The standard mixture for measuring FUT8 activity contained 50 μM of substrate, 200 mM of MES (pH 7.0), 1% Triton X, 500 μM of GDP-Fucose and 23 μL of the plasma sample in a final volume of 50 μL. The reaction mixture was incubated at 37 °C for 6 h, and the reaction was stopped by heating at 100 °C for 1 min. The sample was then centrifuged at 15 000*g* for 10 min, and the supernatant (5 μL) was used for the analysis. The product was separated using high-performance liquid chromatography (HPLC) with a TSK-gel ODS-80TM column (4.6 × 150 mm). Elution was performed at 55 °C with a 20 mM acetate buffer, pH 4.0, containing 0.1% butanol. The fluorescence of the column elute was detected using a fluorescence photometer (HITACHI Fluorescence Spectrophotometer 650−10LC). The excitation and emission wavelengths were observed at 320 and 400 nm, respectively. The product area was used to calculate the enzyme activity (U/L) in all the patients. The enzyme activities were analyzed in duplicate.

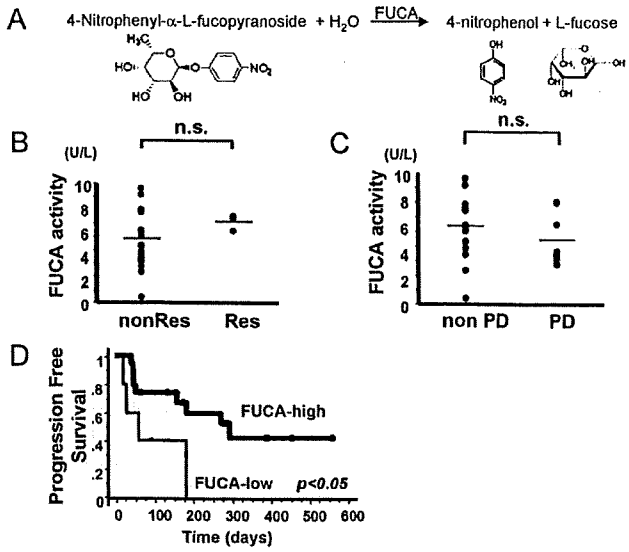

Figure 2. (A) Reaction pathway of α-L fucosidase (FUCA) activity. The substrate (4-nitrophenyl-α-L-fucopyranoside) is defucosylated by FUCA and the products are detected. FUCA activity is measured using spectrophotometer. The enzyme activities were analyzed in duplicate. (B) Plasma FUCA activity and clinical response. Res, responder group (complete response + partial response); nonRes, nonresponder group (stable disease + progressive disease). n.s.: not significant. (C) Plasma FUCA activity and clinical response. PD, progressive disease group; nonPD, nonprogressive disease group. n.s.: not significant. (D) Kaplan–Meier curve for progression-free survival (PFS) of trastuzumab treatment. Patients with a high plasma FUCA activity (4.3 > U/L) exhibited a significantly prolonged PFS ($p < 0.05$).

FUCA Activity Assay. The standard mixture for measuring α-L fucosidase activity contained 20 μL of the plasma sample, 2 mM of 4-nitrophenyl-α-L-fucopyranoside (Sigma, St. Louis, MO), and 50 mM of citrate buffer (pH 4.5) in a final volume of 150 μL in a 96-well microplate. The mixture was incubated at 37 °C for 3 h, and the reaction was stopped by the addition of 100 μL of 0.4 M borate buffer (pH 9.8). The optical density was measured at 405 nm. One unit of enzyme was defined as the amount of enzyme required to produce 1 mmol of product per minute at 37 °C. The enzyme activities were analyzed in duplicate.

Purification of Plasma N-Glycan. Twenty-seven microliters of plasma sample was dissolved in 83 mM ammonium bicarbonate and 10 mM DL-dithiothreitol (Sigma-Aldrich, St. Louis, MO) in a final volume of 60 μL. The mixture was incubated at 60 °C for 30 min, and 10 μL of 123 mM iodoacetamide (Wako Pure Chemicals Co., Tokyo, Japan) was added. After incubation for 1 h at room temperature in the dark, 400 units of trypsin (Sigma-Aldrich) was added to the mixture. The mixture was incubated at 37 °C for 2 h, and the reaction was stopped by heating at 90 °C for 5 min. Five units of peptide *N*-glycosidase F (Roche Diagnostics, Mannheim, Germany) was added, and the mixture was incubated at 37 °C overnight. The internal standard (mannononaose-di-(*N*-acetyl-D-glucosamine), Sigma-Aldrich) was added, and N-glycan was purified from the mixture using BlotGlyco (Sumitomo Bakelite, Co., Tokyo, Japan) according to the manufacture's protocol.[31]

Mass Spectrometry Analysis. The purified samples were concentrated, and 0.5 μL of the sample solution was applied to a sample plate target, then mixed with 0.5 μL of the matrix solution. 2, 5-Dihydroxybenzoic acid (Aldrich) was dissolved in 50% acetonitrile using the matrix solution. After the samples had dried, MALDI-TOF-MS was performed using a Voyager-DE STR Workstation (Applied Biosystems) in reflector, positive ion mode. The number of laser shots was 300 × 2 shots and the mass range acquired was 700–5000 Da. The N-glycan structure was achieved using the GlycoSuite online database, proteome System. The MALDI-TOF-MS spectra data was exported using Voyager Biospectrometry Workstation ver 5.1, Data Explorer Software (Applied Biosystem).

Statistical Analysis. The statistical analyses of the enzyme activity assays and the clinical outcome were performed using the Student's *t*-test by StatView version 5 software (SAS Institute, Inc., Cary, NC). Progression-free survival curves were estimated using the Kaplan–Meier method (StatView). All plasma N-glycans peaks obtained from MALDI-TOF-MS were normalized using an internal standard (mannononaose-di-(*N*-acetyl-D-glucosamine)). The normalized data was imported into BRB Array Tools software ver. 3.3.0 (http://linus.nci.nih.gov/BRB-ArrayTools.html), developed by Dr. Richard Simon and Dr. Amy Peng. N-Glycan peaks were selected for analysis if the peak was observed in over 50% of the patients (>12 patients); finally, 31 peaks of N-glycan were selected. A statistical analysis comparing the N-glycan peaks to response to treatment or PFS was performed. A p-value of <0.05 was considered significant.

Result

Patient Characteristics. Twenty-four patients were evaluated in this study. The mean patient age was 60 years (range 28–76 years). Seventy-one percent (17/24 pts) of the patients had received prior adjuvant chemotherapy, and 58% (14/24 pts) of the patients had received prior radiotherapy. Almost all the patients had a performance status (PS) of 0 or 1 (23/24 pts), and the metastatic sites and hormone receptor status were shown (Table 1). Table 1 summarizes the clinical features of the patients.

Plasma FUT8 Activity and Clinical Outcome. Plasma FUT8 activity was measured using reverse-phase HPLC with a fluorescent substrate (Figure 1A). A representative elution pattern of FUT8 activity in the plasma sample is shown in Figure 1B. The elution times of the substrate and product were 15 and 27 min, respectively. The product area was calculated to determined the overall catalytic activity. The average FUT8 enzyme activity was 2.0 ± 1.3 U/L (average ± SD; range, 0.5 to 5.0 U/L). Regarding the clinical outcome, the FUT8 catalytic activities of responders (CR, complete response; PR, partial response, $n = 3$) and nonresponders (SD, stable disease; PD, progressive disease, $n = 21$) were 1.6 ± 0.7 U/L and 2.0 ± 1.4 U/L, respectively. The activities of the PD and non-PD groups were 1.9 ± 1.2 U/L and 2.0 ± 1.4 U/L, respectivily. No significant correlations between FUT8 activity and the clinical response to trastuzumab were seen (Figure 1C,D). Also, no significant correlations were seen between FUT8 activity and progression-free survival (PFS, data not shown). These results suggest that plasma FUT8 activity is not a useful biomarker for this population.

Correlation of Plasma FUCA Activity and PFS. Plasma FUCA activity was examined using spectrophotometer and 4-nitrophenyl-α-L-fucopyranoside (Figure 2A). The average FUCA enzyme activity was 6.1 ± 2.1 U/L (average ± SD; range, 1.5 to 9.7 U/L). The activities of responders, nonresponders, the PD group and the non-PD group were 7.2 ± 0.6, 5.9 ± 2.2, 5.5 ± 1.8 and 6.3 ± 2.2 U/L, respectively. No significant correlations between FUCA activity and the clinical response to trastuzumab

Table 2. List of Predominant Oligosaccharides in Patient Serum Samples[a]

measured MS (*m/z*)	putative structure
1286.6	ND
1300.6	(Hex)2 (HexNAc)2 (Deoxyhexose)2
1495.5	(Hex)2 + (Man)3(GlcNAc)2
1657.6	(Hex)3 + (Man)3(GlcNAc)2
1701.6	ND
1723.7	(HexNAc)2 (Deoxyhexose)1 + (Man)3(GlcNAc)2
1739.7	(Hex)1 (HexNAc)2 + (Man)3(GlcNAc)2
1841.7	(Hex)1 (HexNAc)1 (NeuAc)1 + (Man)3(GlcNAc)2
1885.7	(Hex)1 (HexNAc)2 (Deoxyhexose)1 + (Man)3(GlcNAc)2
1901.7	(Hex)2 (HexNAc)2 + (Man)3(GlcNAc)2
1926.7	(HexNAc)3 (Deoxyhexose)1 + (Man)3(GlcNAc)2
2047.8	(Hex)2 (HexNAc)2 (Deoxyhexose)1 + (Man)3(GlcNAc)2
2088.8	(Hex)1 (HexNAc)3 (Deoxyhexose)1 + (Man)3(GlcNAc)2
2121.8	(Hex)1 (HexNAc)1 (Deoxyhexose)4 + (Man)3(GlcNAc)2
2206.8	(Hex)2 (HexNAc)2 (NeuAc)1 + (Man)3(GlcNAc)2
2220.8	(HexNAc)3 (Deoxyhexose)3 + (Man)3(GlcNAc)2
2352.9	(Hex)2 (HexNAc)2 (Deoxyhexose)1 (NeuAc)1 + (Man)3(GlcNAc)2
2489.9	(Hex)5 (HexNAc)1 (NeuAc)1 + (Man)3(GlcNAc)2
2493.9	(Hex)1 (HexNAc)5 (Deoxyhexose)1 + (Man)3(GlcNAc)2
2497.9	(Hex)2 (HexNAc)2 (Deoxyhexose)2 (NeuAc)1 + (Man)3(GlcNAc)2
2511.9	(Hex)2 (HexNAc)2 (NeuAc)2 + (Man)3(GlcNAc)2
2519.9	(Hex)4 (HexNAc)2 (Deoxyhexose)2 + (Man)3(GlcNAc)2
2527.9	(Hex)1 (HexNAc)3 (Deoxyhexose)4 + (Man)3(GlcNAc)2
2533.9	(Hex)5 (HexNAc)2 (Deoxyhexose)1 + (Man)3(GlcNAc)2 (Hex)3 (Deoxyhexose)6 + (Man)3(GlcNAc)2
2556.0	(Hex)2 (HexNAc)3 (Deoxyhexose)1 (NeuAc)1 + (Man)3(GlcNAc)2
2572.0	(Hex)3 (HexNAc)3 (NeuAc)1 + (Man)3(GlcNAc)2
2658.0	(Hex)2 (HexNAc)2 (Deoxyhexose)1 (NeuAc)2 + (Man)3(GlcNAc)2
2748.0	(Hex)2 (HexNAc)4 (Deoxyhexose)3 + (Man)3(GlcNAc)2 (Hex)2 (HexNAc)1 (Deoxyhexose)3 (NeuAc)2 + (Man)3(GlcNAc)2
2861.1	(Hex)2 (HexNAc)6 (Deoxyhexose)1 + (Man)3(GlcNAc)2 (Hex)2 (HexNAc)3 (Deoxyhexose)1 (NeuAc)2 + (Man)3(GlcNAc)2
2877.1	(Hex)3 (HexNAc)3 (NeuAc)2 + (Man)3(GlcNAc)2 (Hex)1 (HexNAc)1 (Deoxyhexose)5 (NeuAc)2 + (Man)3(GlcNAc)2
3182.2	(Hex)3 (HexNAc)3 (NeuAc)3 + (Man)3(GlcNAc)2

[a] ND: not determined.

were observed (Figure 2B,C). However, progression-free survival (PFS) was significantly longer in the high FUCA activity group (>4.3 U/L) than in the low FUCA activity group ($p < 0.05$, Figure 2D). Although plasma FUCA activity was not correlated with the clinical response to trastuzumab, it may be useful as a biomarker for predicting the PFS of for trastuzumab treatment.

Low Expression of Plasma 2534 *m/z* N-Glycan Correlated with Unfavorable Clinical Outcome. We collected plasma N-glycans using glycoblotting-based glycan enrichment[31] and measured their MALDI-TOF-MS peaks. Thirty-one major peaks of N-glycan, observed in over 50% of the patients, were identified (Table 2). Representative data are shown in Figure 3 (left panel). A statistical analysis comparing each peak with the clinical outcome revealed that the expression of plasma 2534 *m/z* N-glycan was significantly lower in patients with progressive disease (PD) ($p < 0.05$, Figure 4A). Low expression of 2534 *m/z* N-glycan discriminated between PD and non-PD with 75% sensitivity and 82% specificity. The expressions of plasma 2534 *m/z* N-glycan in the PD and non-PD groups were 4.3 ± 8.1 and 16.1 ± 11.6 (% of control), respectively. Representative data of 2534 *m/z* N-glycan from six patients are shown in Figure 3 (right panel). In addition, patients with a low expression (not detectable at 2534 *m/z*) of plasma 2534 *m/z* N-glycan exhibited a significantly short PFS ($p < 0.05$, Figure 4B). These results suggest that a low plasma 2534 *m/z* N-glycan level is associated with a poor clinical outcome and that plasma 2534 *m/z* N-glycan may be a predictive biomarker in breast cancer patients treated with trastuzumab.

Discussion

In this study, we investigated predictive biomarkers of response to trastuzumab monotherapy in breast cancer patients, focusing on the processes of fucosylation and glycosylation. Shah et al. reported that serum FUCA activity levels varied in normal, precancerous, and malignant conditions, and suggested that serum FUCA activity might be a useful marker for early detection and for monitoring treatment response in oral cancer patients.[32] We found that a higher plasma FUCA activity level was correlated with a favorable PFS, but that the plasma FUT8 levels was not correlated with clinical response and PFS in breast cancer patients who received trastuzumab treatment. Although the precise mechanisms responsible for our results remain unclear, we speculated that the resulting plasma FUT8 level was not correlated with the clinical outcome because FUT8 catalytic activity occurs strictly in the Golgi apparatus and requires GDP-fucose. On the other hand, the FUCA enzyme has two isoforms, FUCA1 (fucosidase, alpha-L-1, tissue) and FUCA2 (fucosidase, alpha-L-2, plasma). Because FUCA2 is secreted into the plasma,[33] it may influence the phenotype of cancer cells, thereby explaining its correlation with clinical outcome. Indeed, the mRNA expression of FUCA2 was higher and that of FUCA1 was lower in biopsy specimens of gastric cancer, compared with paired noncancerous gastric mucosa (data not shown).

Many researchers have reported new methods for performing glycan structural analyses using mass spectrometry.[34,35] Our method of examining N-glycan profiles utilizes only small amount of plasma sample, making it easy to analyze clinical samples. Several reports have demonstrated that analyzing the glycan structures of proteins in human sera can reveal novel tumor markers in cancer.[11,36] Kyselova et al. reported that several N-glycan structures appear to indicate cancer progression in breast cancer, suggesting that N-glycan profiling of serum may be a useful approach for staging the progression of cancer.[37] An et al. reported that oligosaccharide profiling data using sera samples from patients with ovarian cancer patients and normal controls demonstrated the presence of several unique serum glycan markers in all the patients but not in the normal samples.[38] They mentioned that one major advantage of this approarch is that the glycans can be examined

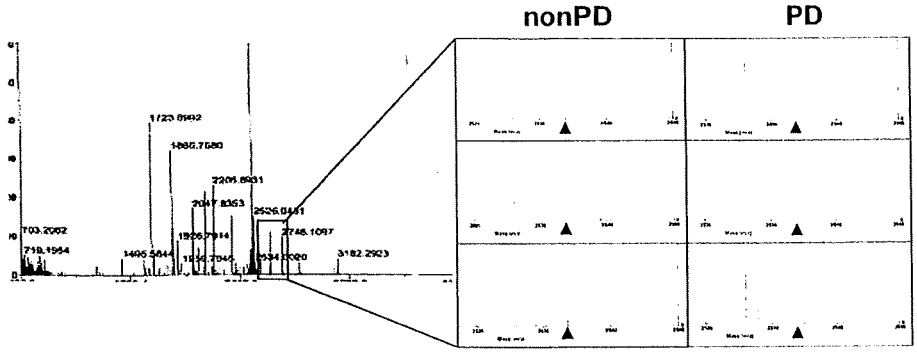

Figure 3. Representative data of plasma N-glycan profile measured using MALDI-TOF-MS (left panel). Twenty-seven microliters of plasma sample was used for the analysis. The mixture was trypsinized and reacted using *N*-glycosidase F. Internal N-glycan standard was added, and the mixture was purified using glycoblotting-based glycan enrichment. The purified samples were measured using MALDI-TOF-MS in reflector, positive ion mode. The number of laser shots was 300 × 2 shots, and the mass range acquired was 700–5000 Da. The N-glycan structure was determined using the GlycoSuite online database, proteome System. All the plasma N-glycans peaks obtained from MALDI-TOF-MS were normalized using the internal standard. The identified 2534 *m/z* N-glycan peaks are shown in six plasma samples (right panel). ▲, 2534 *m/z*; PD, progressive disease.

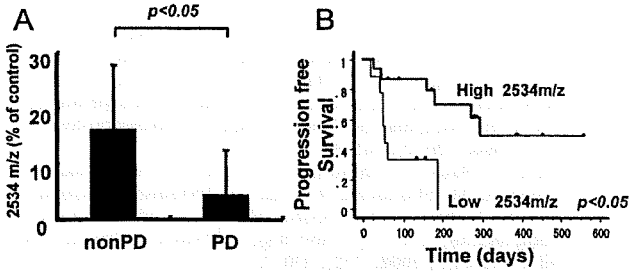

Figure 4. Plasma 2534 *m/z* N-glycan and clinical outcome. (A) Expression of plasma 2534 *m/z* N-glycan and clinical response. The expression of plasma 2534 *m/z* N-glycan was significantly lower ($p < 0.05$) in patients with progressive disease (PD). (B) Kaplan–Meier curve of high (detectable) or low (not detectable) plasma 2534 *m/z* N-glycan groups for progression-free survival (PFS) after trastuzumab treatment. The patients with a low expression of plasma 2534 *m/z* N-glycan exhibited a significantly shorter PFS ($p < 0.05$).

using a serum samples, and cancer biopsy specimens are not needed. In the present study, when the plasma N-glycan profiles of breast cancer patients were examined using MALDI-TOF-MS, 2534 *m/z* N-glycan was found to be correlated with clinical response and PFS. The estimated structure of the identified 2534 *m/z* N-glycan is (Hex)5(HexNAc)2(Deoxyhexose)1 + (Man)3(GlcNAc)2 according to a database (http://au.expasy.org/tools/glycomod/). The experimental confirmation of the predicted structure of 2534 *m/z* is very important. Although we no longer have enough plasma samples to determine the experimental confirmation of structure, we plan to examine 2534 N-glycan in clinical samples to give the experimental confirmation in the future prospective study. This N-glycan has also been found in plasma samples from patients with pancreas cancer, pancreatitis and obstructive bile duct disease (data not shown). We are now investigating the biological mechanism of this N-glycan modification.

In conclusion, we demonstrated that plasma FUCA activity and plasma N-glycan are correlated with the clinical outcome of breast cancer patients treated with trastuzumab. N-Glycan profiles raise the possibility of identifying novel predictive biomarkers for antibody therapy, although a validation study with a larger sample size is needed. Our results show the utility of glycosylation analysis for clinical cancer therapy and provide a novel insight into biomarker studies using glycobiological tools in the field of breast cancer.

Acknowledgment. The following people have played very important roles in the outcome of this project: Hisao Fukumoto, Tatsu Shimoyama, Naoki Hayama, Hideharu Kimura, Masayuki Takeda, Junya Fukai, Kazuko Sakai and Terufumi Kato. We also thank Dr. Richard Simon and Dr. Amy Peng for providing the BRB ArrayTools software. We thank Mr. Hideyuki Shimaoka and Mr. Kazuhiko Fujiwara (Sumitomo Bakelite Co., Ltd.) for their technical support and useful advice. We also thank Mrs. Eiko Honda (Life Science Research Institute, Kinki University) for assistance with the experiments. This work was supported by funds for Health and Labor Scientific Research Grants, Research on Advanced Medical Technology H17-Pharmaco-006 and for the Third-Term Comprehensive 10-Year Strategy for Cancer Control. K.M. is the recipient of a Research Resident Fellowship from the Foundation of Promotion of Cancer Research in Japan.

References

(1) Hakomori, S. Glycosylation defining cancer malignancy: new wine in an old bottle. *Proc. Natl. Acad. Sci. U.S.A.* **2002**, *99* (16), 10231–3.
(2) Ono, M.; Hakomori, S. Glycosylation defining cancer cell motility and invasiveness. *Glycoconjugate J.* **2004**, *20* (1), 71–8.
(3) Zhao, Y. Y.; Takahashi, M.; Gu, J. G.; Miyoshi, E.; Matsumoto, A.; Kitazume, S.; Taniguchi, N. Functional roles of N-glycans in cell signaling and cell adhesion in cancer. *Cancer Sci.* **2008**, *99* (7), 1304–10.
(4) Hakomori, S. Tumor malignancy defined by aberrant glycosylation and sphingo(glyco)lipid metabolism. *Cancer Res.* **1996**, *56* (23), 5309–18.
(5) Contessa, J. N.; Bhojani, M. S.; Freeze, H. H.; Rehemtulla, A.; Lawrence, T. S. Inhibition of N-linked glycosylation disrupts receptor tyrosine kinase signaling in tumor cells. *Cancer Res.* **2008**, *68* (10), 3803–9.
(6) Guo, H. B.; Randolph, M.; Pierce, M. Inhibition of a specific N-glycosylation activity results in attenuation of breast carcinoma cell invasiveness-related phenotypes: inhibition of epidermal growth factor-induced dephosphorylation of focal adhesion kinase. *J. Biol. Chem.* **2007**, *282* (30), 22150–62.
(7) Qiu, Y.; Patwa, T. H.; Xu, L.; Shedden, K.; Misek, D. E.; Tuck, M.; Jin, G.; Ruffin, M. T.; Turgeon, D. K.; Synal, S.; Bresalier, R.; Marcon, N.; Brenner, D. E.; Lubman, D. M. Plasma glycoprotein profiling for colorectal cancer biomarker identification by lectin glycoarray and lectin blot. *J. Proteome Res.* **2008**, *7* (4), 1693–703.

(8) Abbott, K. L.; Aoki, K.; Lim, J. M.; Porterfield, M.; Johnson, R.; O'Regan, R. M.; Wells, L.; Tiemeyer, M.; Pierce, M. Targeted glycoproteomic identification of biomarkers for human breast carcinoma. *J. Proteome Res.* **2008**, *7* (4), 1470–80.
(9) Heo, S. H.; Lee, S. J.; Ryoo, H. M.; Park, J. Y.; Cho, J. Y. Identification of putative serum glycoprotein biomarkers for human lung adenocarcinoma by multilectin affinity chromatography and LC-MS/MS. *Proteomics* **2007**, *7* (23), 4292–302.
(10) Nakagawa, T.; Uozumi, N.; Nakano, M.; Mizuno-Horikawa, Y.; Okuyama, N.; Taguchi, T.; Gu, J.; Kondo, A.; Taniguchi, N.; Miyoshi, E. Fucosylation of N-glycans regulates the secretion of hepatic glycoproteins into bile ducts. *J. Biol. Chem.* **2006**, *281* (40), 29797–806.
(11) Ueda, K.; Katagiri, T.; Shimada, T.; Irie, S.; Sato, T. A.; Nakamura, Y.; Daigo, Y. Comparative profiling of serum glycoproteome by sequential purification of glycoproteins and 2-nitrobenzensulfenyl (NBS) stable isotope labeling: a new approach for the novel biomarker discovery for cancer. *J. Proteome Res.* **2007**, *6* (9), 3475–83.
(12) Li, D.; Mallory, T.; Satomura, S. AFP-L3: a new generation of tumor marker for hepatocellular carcinoma. *Clin. Chim. Acta* **2001**, *313* (1–2), 15–9.
(13) Yamaguchi, Y.; Fujii, J.; Inoue, S.; Uozumi, N.; Yanagidani, S.; Ikeda, Y.; Egashira, M.; Miyoshi, O.; Niikawa, N.; Taniguchi, N. Mapping of the alpha-1,6-fucosyltransferase gene, FUT8, to human chromosome 14q24.3. *Cytogenet. Cell Genet.* **1999**, *84* (1–2), 58–60.
(14) Yamane-Ohnuki, N.; Kinoshita, S.; Inoue-Urakubo, M.; Kusunoki, M.; Iida, S.; Nakano, R.; Wakitani, M.; Niwa, R.; Sakurada, M.; Uchida, K.; Shitara, K.; Satoh, M. Establishment of FUT8 knockout Chinese hamster ovary cells: an ideal host cell line for producing completely defucosylated antibodies with enhanced antibody-dependent cellular cytotoxicity. *Biotechnol. Bioeng.* **2004**, *87* (5), 614–22.
(15) Niwa, R.; Hatanaka, S.; Shoji-Hosaka, E.; Sakurada, M.; Kobayashi, Y.; Uehara, A.; Yokoi, H.; Nakamura, K.; Shitara, K. Enhancement of the antibody-dependent cellular cytotoxicity of low-fucose IgG1 Is independent of FcgammaRIIIa functional polymorphism. *Clin. Cancer Res.* **2004**, *10* (18 Pt 1), 6248–55.
(16) Suzuki, E.; Niwa, R.; Saji, S.; Muta, M.; Hirose, M.; Iida, S.; Shiotsu, Y.; Satoh, M.; Shitara, K.; Kondo, M.; Toi, M. A nonfucosylated anti-HER2 antibody augments antibody-dependent cellular cytotoxicity in breast cancer patients. *Clin. Cancer Res.* **2007**, *13* (6), 1875–82.
(17) Giardina, M. G.; Matarazzo, M.; Morante, R.; Lucariello, A.; Varriale, A.; Guardasole, V.; De Marco, G. Serum alpha-L-fucosidase activity and early detection of hepatocellular carcinoma: a prospective study of patients with cirrhosis. *Cancer.* **1998**, *83* (12), 2468–74.
(18) Ayude, D.; Paez De La Cadena, M.; Martinez-Zorzano, V. S.; Fernandez-Briera, A.; Rodriguez-Berrocal, F. J. Preoperative serum alpha-L-fucosidase activity as a prognostic marker in colorectal cancer. *Oncology* **2003**, *64* (1), 36–45.
(19) Ayude, D.; Fernandez-Rodriguez, J.; Rodriguez-Berrocal, F. J.; Martinez-Zorzano, V. S.; de Carlos, A.; Gil, E.; Paez de La Cadena, M. Value of the serum alpha-L-fucosidase activity in the diagnosis of colorectal cancer. *Oncology* **2000**, *59* (4), 310–6.
(20) Slamon, D. J.; Clark, G. M.; Wong, S. G.; Levin, W. J.; Ullrich, A.; McGuire, W. L. Human breast cancer: correlation of relapse and survival with amplification of the HER-2/neu oncogene. *Science* **1987**, *235* (4785), 177–82.
(21) Seshadri, R.; Firgaira, F. A.; Horsfall, D. J.; McCaul, K.; Setlur, V.; Kitchen, P. Clinical significance of HER-2/neu oncogene amplification in primary breast cancer. The South Australian Breast Cancer Study Group. *J Clin Oncol.* **1993**, *11* (10), 1936–42.
(22) Menard, S.; Pupa, S. M.; Campiglio, M.; Tagliabue, E. Biologic and therapeutic role of HER2 in cancer. *Oncogene* **2003**, *22* (42), 6570–8.
(23) Vogel, C. L.; Cobleigh, M. A.; Tripathy, D.; Gutheil, J. C.; Harris, L. N.; Fehrenbacher, L.; Slamon, D. J.; Murphy, M.; Novotny, W. F.; Burchmore, M.; Shak, S.; Stewart, S. J.; Press, M. Efficacy and safety of trastuzumab as a single agent in first-line treatment of HER2-overexpressing metastatic breast cancer. *J. Clin. Oncol.* **2002**, *20* (3), 719–26.
(24) Hurley, J.; Doliny, P.; Reis, I.; Silva, O.; Gomez-Fernandez, C.; Velez, P.; Pauletti, G.; Powell, J. E.; Pegram, M. D.; Slamon, D. J. Docetaxel, cisplatin, and trastuzumab as primary systemic therapy for human epidermal growth factor receptor 2-positive locally advanced breast cancer. *J. Clin. Oncol.* **2006**, *24* (12), 1831–8.
(25) Naruse, I.; Fukumoto, H.; Saijo, N.; Nishio, K. Enhanced anti-tumor effect of trastuzumab in combination with cisplatin. *Jpn. J. Cancer Res.* **2002**, *93* (5), 574–81.
(26) Kimura, H.; Sakai, K.; Arao, T.; Shimoyama, T.; Tamura, T.; Nishio, K. Antibody-dependent cellular cytotoxicity of cetuximab against tumor cells with wild-type or mutant epidermal growth factor receptor. *Cancer Sci.* **2007**, *98* (8), 1275–80.
(27) Kimura, H.; Kasahara, K.; Kawaishi, M.; Kunitoh, H.; Tamura, T.; Holloway, B.; Nishio, K. Detection of epidermal growth factor receptor mutations in serum as a predictor of the response to gefitinib in patients with non-small-cell lung cancer. *Clin. Cancer Res.* **2006**, *12* (13), 3915–21.
(28) Arao, T.; Fukumoto, H.; Takeda, M.; Tamura, T.; Saijo, N.; Nishio, K. Small in-frame deletion in the epidermal growth factor receptor as a target for ZD6474. *Cancer Res.* **2004**, *64* (24), 9101–4.
(29) Matsumoto, K.; Yokote, H.; Arao, T.; Maegawa, M.; Tanaka, K.; Fujita, Y.; Shimizu, C.; Hanafusa, T.; Fujiwara, Y.; Nishio, K. N-Glycan fucosylation of epidermal growth factor receptor modulates receptor activity and sensitivity to epidermal growth factor receptor tyrosine kinase inhibitor. *Cancer Sci.* **2008**, *99* (8), 1611–17.
(30) Uozumi, N.; Teshima, T.; Yamamoto, T.; Nishikawa, A.; Gao, Y. E.; Miyoshi, E.; Gao, C. X.; Noda, K.; Islam, K. N.; Ihara, Y.; Fujii, S.; Shiba, T.; Taniguchi, N. A fluorescent assay method for GDP-L-Fuc:N-acetyl-beta-D-glucosaminide alpha 1−6fucosyltransferase activity, involving high performance liquid chromatography. *J. Biochem.* **1996**, *120* (2), 385–92.
(31) Miura, Y.; Hato, M.; Shinohara, Y.; Kuramoto, H.; Furukawa, J.; Kurogochi, M.; Shimaoka, H.; Tada, M.; Nakanishi, K.; Ozaki, M.; Todo, S.; Nishimura, S. BlotGlycoABCTM, an integrated glycoblotting technique for rapid and large scale clinical glycomics. *Mol. Cell. Proteomics* **2008**, *7* (2), 370–7.
(32) Shah, M.; Telang, S.; Raval, G.; Shah, P.; Patel, P. S. Serum fucosylation changes in oral cancer and oral precancerous conditions: alpha-L-fucosidase as a marker. *Cancer* **2008**, *113* (2), 336–46.
(33) Ng, W. G.; Donnell, G. N.; Koch, R.; Bergren, W. R. Biochemical and genetic studies of plasma and leukocyte alpha-L-fucosidase. *Am. J. Hum. Genet.* **1976**, *28* (01), 42–50.
(34) Zhao, J.; Qiu, W.; Simeone, D. M.; Lubman, D. M. N-linked glycosylation profiling of pancreatic cancer serum using capillary liquid phase separation coupled with mass spectrometric analysis. *J. Proteome Res.* **2007**, *6* (3), 1126–38.
(35) Zhao, J.; Simeone, D. M.; Heidt, D.; Anderson, M. A.; Lubman, D. M. Comparative serum glycoproteomics using lectin selected sialic acid glycoproteins with mass spectrometric analysis: application to pancreatic cancer serum. *J. Proteome Res.* **2006**, *5* (7), 1792–802.
(36) Isailovic, D.; Kurulugama, R. T.; Plasencia, M. D.; Stokes, S. T.; Kyselova, Z.; Goldman, R.; Mechref, Y.; Novotny, M. V.; Clemmer, D. E. Profiling of human serum glycans associated with liver cancer and cirrhosis by IMS-MS. *J. Proteome Res.* **2008**, *7* (3), 1109–17.
(37) Kyselova, Z.; Mechref, Y.; Kang, P.; Goetz, J. A.; Dobrolecki, L. E.; Sledge, G. W.; Schnaper, L.; Hickey, R. J.; Malkas, L. H.; Novotny, M. V. Breast cancer diagnosis and prognosis through quantitative measurements of serum glycan profiles. *Clin Chem.* **2008**, *54* (7), 1166–75.
(38) An, H. J.; Miyamoto, S.; Lancaster, K. S.; Kirmiz, C.; Li, B.; Lam, K. S.; Leiserowitz, G. S.; Lebrilla, C. B. Profiling of glycans in serum for the discovery of potential biomarkers for ovarian cancer. *J. Proteome Res.* **2006**, *5* (7), 1626–35.

PR800655P

Epidermal growth factor receptor lacking C-terminal autophosphorylation sites retains signal transduction and high sensitivity to epidermal growth factor receptor tyrosine kinase inhibitor

Mari Maegawa,[1,2] Tokuzo Arao,[1] Hideyuki Yokote,[1] Kazuko Matsumoto,[1] Kanae Kudo,[1] Kaoru Tanaka,[1] Hiroyasu Kaneda,[1] Yoshihiko Fujita,[1] Fumiaki Ito[2] and Kazuto Nishio[1,3]

[1]Department of Genome Biology, Kinki University School of Medicine, 377-2 Ohno-Higashi, Osaka Sayama, Osaka, 589-8511; [2]Department of Biochemistry, Setsunan University, 45-1 Nagaotoge-cho Hirakata, Osaka, 573-0101 Japan

(Received September 30, 2008/Revised November 19, 2008/Accepted November 29, 2008)

Constitutively active mutations of epidermal growth factor receptor (EGFR) (delE746_A750) activate downstream signals, such as ERK and Akt, through the phosphorylation of tyrosine residues in the C-terminal region of EGFR. These pathways are thought to be important for cellular sensitivity to EGFR tyrosine kinase inhibitors (TKI). To examine the correlation between phosphorylation of the tyrosine residues in the C-terminal region of EGFR and cellular sensitivity to EGFR TKI, we used wild-type (wt) EGFR, as well as the following constructs: delE746_A750 EGFR; delE746_A750 EGFR with substitution of seven tyrosine residues to phenylalanine in the C-terminal region; and delE746_A750 EGFR with a C-terminal truncation at amino acid 980. These constructs were transfected stably into HEK293 cells and designated HEK293/Wt, HEK293/D, HEK293/D7F, and HEK293/D-Tr, respectively. The HEK293/D cells were found to be 100-fold more sensitive to EGFR TKI (AG1478) than HEK293/Wt. Surprisingly, the HEK293/D7F and HEK293/D-Tr cells, transfected with EGFR lacking the C-terminal autophosphorylation sites, retained high sensitivity to EGFR TKI. In these three high-sensitivity cells, the ERK pathway was activated without ligand stimulation, which was inhibited by EGFR TKI. In addition, although EGFR in the HEK293/D7F and HEK293/D-Tr cells lacked significant tyrosine residues for EGFR signal transduction, phosphorylation of Src homology and collagen homology (Shc) was spontaneously activated in these cells. Our results indicate that tyrosine residues in the C-terminal region of EGFR are not required for cellular sensitivity to EGFR TKI, and that an as-yet-unknown signaling pathway of EGFR may exist that is independent of the C-terminal region of EGFR. (*Cancer Sci* 2009)

Epidermal growth factor receptor (EGFR), also termed HER1/ErbB-1, is overexpressed and activated in many cancers.[1–3] Small-molecule inhibitors of EGFR tyrosine kinase and antibodies have been shown to exhibit antitumor activity in several tumors.[4–6] Somatic mutations of EGFR tyrosine kinase in non-small cell lung cancer have been shown to be associated with hyperresponsiveness to gefitinib, a selective EGFR tyrosine kinase inhibitor (TKI).[7,8] Many investigators have subsequently reported that EGFR mutations are strong determinants of the tumor response to EGFR TKI.[9,10] Approximately 90% of non-small cell lung cancer-associated EGFR mutations in two reports consisted of two major EGFR mutations, namely, delE746_A750 in exon 19 and L858R in exon 21.[11] We previously reported hypersensitivity to EGFR TKI of a PC-9 cell line with delE746_A750 in exon 19, one of the commonly encountered mutations mentioned above, and this deletion mutant of EGFR was constitutively active and activated the ERK and Akt pathway.[12–16] Binding of the receptor with its ligand leads to homodimerization and heterodimerization of the receptor tyrosine kinase.[17,18] Thus, EGFR is a ligand-activated tyrosine kinase that ultimately delivers cellular growth signals.

Tyr-1068, Tyr-1148, and Tyr-1173 in the C-terminal region are the major autophosphorylation sites in human EGFR. These C-terminal phosphorylation sites of EGFR interact with adaptor proteins.[19,20] Phosphorylation of the C-terminal autophosphorylation sites of EGFR, triggered by epidermal growth factor (EGF), in turn trigger an intracellular signal cascade involving proteins such as ERK, Akt, Janus kinase, and signal transducer and activator of transcription.[15,21,22] Src homology and collagen homology (Shc) is a molecular adaptor protein that binds phosphorylated tyrosines within activated EGFR, and is itself phosphorylated on tyrosine residues upon stimulation of EGFR. The phosphorylated CH1 site of Shc then engages the binding site for the SH2 domain of growth factor receptor-bound protein (Grb) 2. The SH3 domain of Grb2 directly interacts with the guanyl nucleotide exchange factor son of sevenless homolog (Sos).[23,24] Sos catalyzes the conversion of GDP to GTP on Ras, resulting in Ras activation. Activated GTP-Ras recruits Raf kinase to the plasma membrane, resulting in Raf activation and phosphorylation of its downstream target ERK kinase.[25,26]

Phosphorylation of tyrosine residues at the C-terminal region of EGFR is believed to be important in cell signaling triggered by wild-type EGFR.[27,28] However, the role of this region in an active mutant of EGFR (delE746_A750) has yet to be elucidated in detail. To clarify the biological functions of the tyrosine residues at the C-terminal region of EGFR, we constructed several mutants with C-terminal-truncated or substitution of tyrosine residues to phenylalanine in the C-terminal region. We showed that EGFR lacking C-terminal autophosphorylation sites still generated signals, with retention of cellular hypersensitivity to EGFR TKI.

Materials and Methods

Expression constructs. The method used to obtain full-length cDNA of wild-type *EGFR* has been described previously.[12] Wild-type *EGFR* cDNA and 15 bp-deletion *EGFR* (delE746_A750) were introduced into pcDNA3.1 (Invitrogen, Carlsbad, CA, USA) with a myc-tag at its C-terminus. The *EGFR* cDNA with substitution of seven tyrosine residues to phenylalanine in the C-terminal region was amplified by mutagenesis; the QuikChange®

[3]To whom correspondence should be addressed. E-mail: knishio med.kindai.ac.jp

doi: 10.1111/j.1349-7006.2008.01071.x

Site-Directed Mutagenesis Kit (Stratagene, La Jolla, CA, USA) was used for the polymerase chain reaction and a primer set was synthesized (Supporting Information Table S1). The cDNA of the C-terminal-truncated *EGFR* with 15-bp deletion (*EGFR-D-Tr*) was amplified using the following primer set: forward, CCT CCT CTT GCT GCT GGT GGT G; reverse, GAA CAAGCT TGA CAA GGT AGC GCT GGG GGT CTC. After the polymerase chain reaction products were cut with *Cla*I and *Hind*III, they were ligated to the *Cla*I and *Hind*III sites of the pcDNA3.1 expression vector containing EGFR-D cDNA. The cDNA of wild-type *EGFR* with the C-terminal truncation at amino acid 980 (*EGFR-Wt-Tr*) was made from the *Cla*I and *Xho*I fragments of the pcDNA3.1 expression vector containing wild-type EGFR and the *Cla*I and *Xho*I fragments of the pcDNA3.1 expression vector containing *EGFR-D-Tr*.

Epidermal growth factor receptor cDNA with the myc-tag in pcDNA3.1 was cut and introduced into a pQCLIN retroviral vector (BD Biosciences Clontech, San Diego, CA, USA) together with enhanced green fluorescent protein (EGFP) followed by the internal ribosome entry sequence, to monitor the expression of the inserts indirectly. A pVSV-G vector (Clontech, Palo Alto, CA, USA) for constitution of the viral envelope, pGP vector (Takara, Yotsukaichi, Japan), and the pQCXIX constructs were cotransfected into HEK293 cells using FuGENE6 transfection reagent (Roche Diagnostics, Basel, Switzerland). Briefly, 80% confluent cells cultured in a 10-cm dish were transfected with 2 μg pVSV-G vector plus 6 μg pQCXIX vector. Forty-eight hours after the transfection, the culture medium was collected and the viral particles were concentrated by centrifugation at 15 000*g* for 3 h at 4°C. The viral pellet was then resuspended in fresh Dulbecco's modified Eagle's medium (DMEM; Sigma, St Louis, MO, USA). The titer of the viral vector was calculated by counting the EGFP-positive cells that were infected in serial dilutions of a virus-containing medium and then determining the multiplicity of infection. HER2 and HER3 introduced retrovirally into HEK293 cells were used as positive controls in western blotting.

Cell culture and transfection. The human embryonic kidney HEK293 cell line was obtained from the American Type Culture Collection (Manassas, VA, USA) and cultured in DMEM supplemented with 10% fetal bovine serum, penicillin, and streptomycin (Sigma) in a humidified atmosphere of 5% CO_2 at 37°C. The HEK293 cells were transfected with the viral vectors.

***In vitro* growth-inhibition assay.** The growth-inhibitory effects of AG1478 (Biomol International, Plymouth Meeting, PA, USA) in HEK293/Wt, HEK293/Wt-Tr, HEK293/D, HEK293/D7F, and HEK293/D-Tr cells were examined using a 3, 4, 5-dimethyl-2H-tetrazolium bromide (MTT) assay as described previously.[29]

Immunoprecipitation. The culture cells were washed twice with ice-cold phosphate-buffered saline (PBS) (–), and lysed with a lysis buffer containing 20 mM Tris-HCl (pH 7.0), 50 mM NaCl, 5 mM ethylenediaminetetraacetic acid, 10 mM Na pyrophosphate, 50 mM NaF, 1 mM Na orthovanadate, 1% TritonX-100, and the Complete Mini protease inhibitor mix (Roche Diagnostics). The lysates were cleared by centrifugation at 15 000 *g* for 10 min and the protein concentrations of the supernatants were measured using a bicinchoninic acid protein assay (Pierce Biotechnology, Rockford, IL, USA).

The cell lysates (500 μg) were immunoprecipitated by overnight incubation with 3 μg anti-EGFR antibody, anti-HER3 antibody (Upstate Biotechnology, Lake Placid, NY, USA), anti-HER2 antibody (Santa Cruz Biotechnology, Santa Cruz, CA), or anti-c-Myc (Roche Diagnostics), followed by further incubation with protein-G agarose (Santa Cruz Biotechnology) for 1 h. Bound proteins were washed three times with lysis buffer and eluted in Laemmli sample buffer containing 2-mercaptoethanol. The eluted proteins were subjected to 2–15% gradient sodium dodecylsulfate–polyacrylamide gel electrophoresis (SDS-PAGE) and immmunoblotted as described above.

Immunoblotting. Whole-cell lysates and the immunoprecipitates were separated using 2–15% gradient SDS-PAGE and blotted on to a polyvinylidene fluoride membrane. The membrane was probed with anti-EGFR, anti-HER3 (Upstate Biotechnology), anti-phospho(Tyr845)-EGFR, anti-phospho(Tyr1068)-EGFR, anti-phospho(Tyr1173)-EGFR, anti-HER2, anti-phospho-tyrosine, anti-p44/42 mitogen-activated protein (MAP) kinase, anti-phospho-p44/42 MAP kinase, anti-Shc, anti-phospho-Shc (Cell Signaling, Beverly, MA), anti-Sos (Santa Cruz), anti-Grb2 (BD Biosciences, San Jose, CA), and anti-c-Myc (Roche Diagnostics) antibodies by incubation for 2 h at room temperature and then with horseradish peroxidase-conjugated anti-rabbit IgG antibody or anti-mouse IgG antibody for 1 h at room temperature. Finally, the proteins were visualized with an enhanced chemiluminescence western blotting detection system (GE Healthcare, Piscataway, NJ, USA).

Chemical crosslinking assay. After treatment or no treatment with EGF (R&D Systems, Minneapolis, MN, USA) the chemical crosslinking assay was carried out in intact cells as described previously.[13] The transfected cells were washed with ice-cold PBS (+) and incubated for 30 min at room temperature in PBS (+) containing 2 mM crosslinker bis(sulfosuccinimidyl)suberate (Pierce Biotechnology). The reaction was terminated with 20 mM Tris (pH 7.5) for 15 min at room temperature. The cells were washed with PBS (+), and 15 μg protein was resolved by 2–15% gradient SDS-PAGE and then immunoblotted with anti-EGFR and anti-phospho-EGFR antibodies.

Results

Epidermal growth factor receptor lacking C-terminal autophosphorylation sites (EGFR-D-Tr and EGFR-D7F) retains signal transduction. To examine the role of the tyrosine residues in the C-terminal region of EGFR in signal transduction, we constructed vectors containing wild-type EGFR, a deletion mutant (delE746_A750 EGFR) with C-terminal truncation, or a mutant with substitution of seven tyrosine residues in the C-terminal region (Fig. 1a), and transfected these vectors into HEK293 cells with rather low expression levels of endogenous EGFR. The expression of exogenous EGFR in the transfectants was confirmed by immunoblotting with anti-EGFR antibodies (Fig. 1b).

In order to examine the signal transduction of EGFR in the transfectants, we analyzed the phosphorylation status of EGFR and its downstream molecules. Phosphorylation of EGFR at the Y845 and Y1173 tyrosine residues was detected in HEK293/Wt and HEK293/D cells cultivated in medium containing 10% fetal bovine serum (Fig. 2a). Enhanced phosphorylation of the Y1068 tyrosine residue was observed specifically in the HEK293/D cells, suggesting that Y1068 is constitutively active in delE746_A750 EGFR. This phenomenon is consistent with our previous reports.[29,30] On the other hand, no significant phosphorylation of Y845, Y1068, or Y1173 was observed in the HEK293/D7F and HEK293/D-Tr cells. ERK and Akt are major downstream pathways of EGFR. We examined the phosphorylation of ERK and Akt in the transfectants. Increased phosphorylation of ERK was observed in the HEK293/D7F, HEK293/D-Tr, and HEK293/D cells, even though HEK293/D7F and HEK293/D-Tr cells were transfected with EGFR lacking the C-terminal autophosphorylation sites.

We also examined ligand-dependent signals in these cells under the 1% serum starve medium (Fig. 2b). Ligand-stimulated phosphorylation of EGFR was observed in the HEK293/Wt cells transfected with wild-type EGFR. Constitutive phosphorylation of EGFR and a further increase in the EGFR phosphorylation response to EGF were observed in the HEK293/D cells. On the other hand, no significant phosphorylation in response to EGF binding was observed in the HEK293/D7F and HEK293/D-Tr cells. Downstream of EGFR, increased phosphorylation of ERK and Akt was observed in response to EGF in the HEK293/D7F

doi: 10.1111/j.1349-7006.2008.01071.x

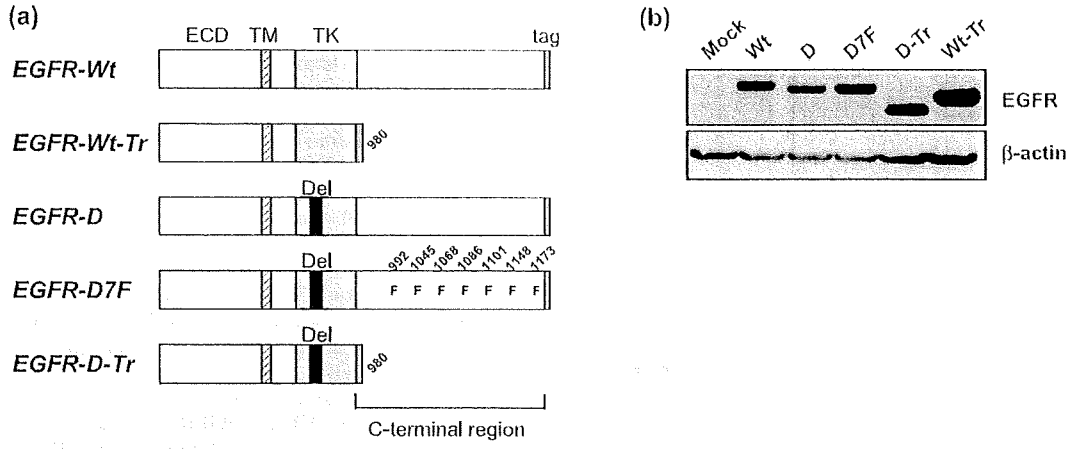

Fig. 1. Epidermal growth factor receptor (EGFR) constructs and their expression. (a) Structures of the various EGFR mutants. EGFR-Wt, wild-type human EGFR; EGFR-Wt-Tr, wild-type kinase domain of EGFR with C-terminal truncation at amino acid 980; EGFR-D, EGFR with a 15-bp deletion from the tyrosine kinase domain (delE746_A750); EGFR-D7F, 15-bp deletion of EGFR (delE746_A750) and substitution of seven tyrosine residues to phenylalanine (Y992F, Y1068F, Y1045F, Y1068F, Y1086F, Y1148F, Y1173F); and EGFR-D-Tr, 15-bp deletion of EGFR (delE746_A750) with C-terminal truncation at amino acid 980. EGFR-Wt, EGFR-D, EGFR-D7F, and EGFR-D-Tr contained a myc-tag. EGFR-Wt-Tr contained a flag-tag. ECD, extracellular domain; TK, tyrosine kinase; TM, transmembrane. (b) Stable transfectants were lysed and cell lysates containing equal amounts of protein were immunoblotted with anti-EGFR antibody recognizing the extracellular domain of EGFR. A band with a molecular weight of ~170 kDa was detected in the HEK293/Wt, HEK293/D, and HEK293/D7F cells, and a band of lower molecular weight was detected in the HEK293/D-Tr and HEK293/Wt-Tr cells. Mock, HEK293/Mock; Wt, HEK293/Wt; Wt-Tr, HEK293/Wt-Tr; D, HEK293/D; D7F, HEK293/D7F; and D-Tr, HEK293/D-Tr.

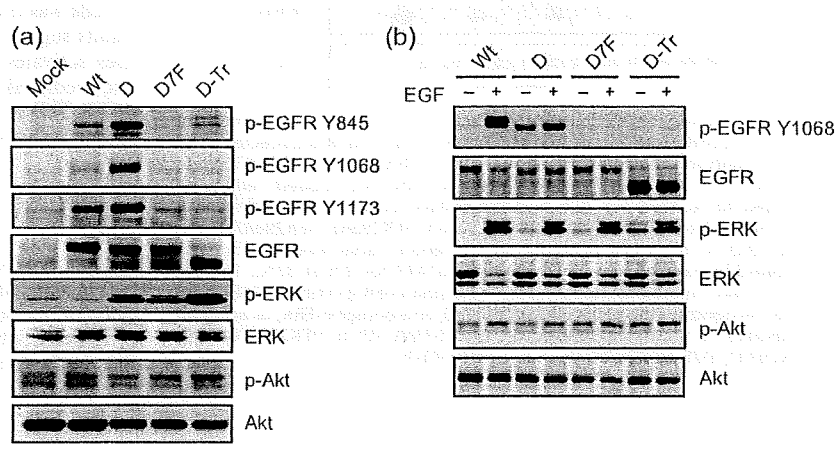

Fig. 2. Epidermal growth factor receptor (EGFR) lacking C-terminal autophosphorylation sites retains EGFR signal transduction. (a) The HEK293/Mock, HEK293/Wt, HEK293/D, HEK293/D7F, and HEK293/D-Tr cells were lysed, and the cell lysates were immunoblotted with anti-phospho-EGFR (p-EGFR Y845, Y1068, Y1173), anti-EGFR (recognizing the extracellular domain), anti-phospho-ERK, anti-ERK, anti-phospho-Akt, and anti-Akt antibodies. (b) The HEK293/Wt, HEK293/D, HEK293/D7F, and HEK293/D-Tr cells were incubated in 1% serum starve medium for 12 h, followed by treatment with 10 ng/mL epidermal growth factor for 10 min at 37°C. The cell lysates were immunoblotted. Mock, HEK293/Mock; Wt, HEK293/Wt; D, HEK293/D; D7F, HEK293/D7F; and D-Tr, HEK293/D-Tr.

and HEK293/D-Tr cells, as well as the HEK293/Wt and HEK293/D cells. These results indicate that EGFR lacking the C-terminal autophosphorylation sites (EGFR-D-Tr and EGFR-D7F) retained signal transduction ability.

Transfectants with EGFR lacking C-terminal autophosphorylation sites retain their hypersensitivity to EGFR TKI. EGF stimulation increased the growth of HEK293/Wt cells significantly but did not affect their sensitivity to AG1478 (data not shown). To examine the role of the C-terminal region of EGFR in cellular sensitivity to EGFR TKI, the sensitivity of these transfectants was examined by growth-inhibition assay (Fig. 3a). HEK293/Wt and HEK293/Wt-Tr cells with normal EGFR in relation to the kinase domain were relatively resistant to EGFR TKI, with IC_{50} values of 3.0 ± 0.97 and 8.1 ± 0.99 μM. On the other hand, HEK293/D (0.028 ± 0.018 μM), HEK293/D7F (0.047 ± 0.030 μM), and HEK293/D-Tr (0.017 ± 0.017 μM) cells were ~100 times more sensitive to AG1478 compared to HER293/Wt cells (Fig. 3a), suggesting that the cells transfected with EGFR lacking C-terminal phosphorylation sites retained hypersensitivity to EGFR TKI. There were no differences in the proliferation rates of these cell lines under the absence of drug exposure (data not shown).

To elucidate the effect of EGFR TKI on the EGFR-triggered signal cascade, the phosphorylation status of EGFR and ERK was examined in the transfectants treated with AG1478 under the 1% serum starve medium (Fig. 3b). AG1478 at a concentration of 20 nM inhibited the phosphorylation of EGFR in HEK293/D cells, but not in the other cell lines. The increased phosphorylation of ERK observed in the HEK293/D, HEK293/D7F, and HEK293/D-Tr cells was inhibited by AG1478 at 20 nM. These results suggest that signal transduction from C-terminal-truncated EGFR to downstream molecules allows sensitivity to EGFR TKI to be retained, just like the deletion mutant of EGFR (delE746_A750).

Endogenous HER families are not involved in the dimerization of EGFR-D-Tr and EGFR-D7F. We hypothesized that the signals from EGFR lacking the C-terminal autophosphorylation sites were transduced through heterodimerization with endogenous EGFR, HER2, or HER3. No significant endogenous EGFR expression or its phosphorylation was observed in the HEK293/Mock cells (Fig. 4a). Very low levels of intrinsic HER2 or HER3 expression were detected in the HEK293 cells, and the expression levels seemed not to be involved in significant drug sensitivity nor increased signal transduction (Fig. 4b,c). Therefore, it is not likely that heterodimerization of

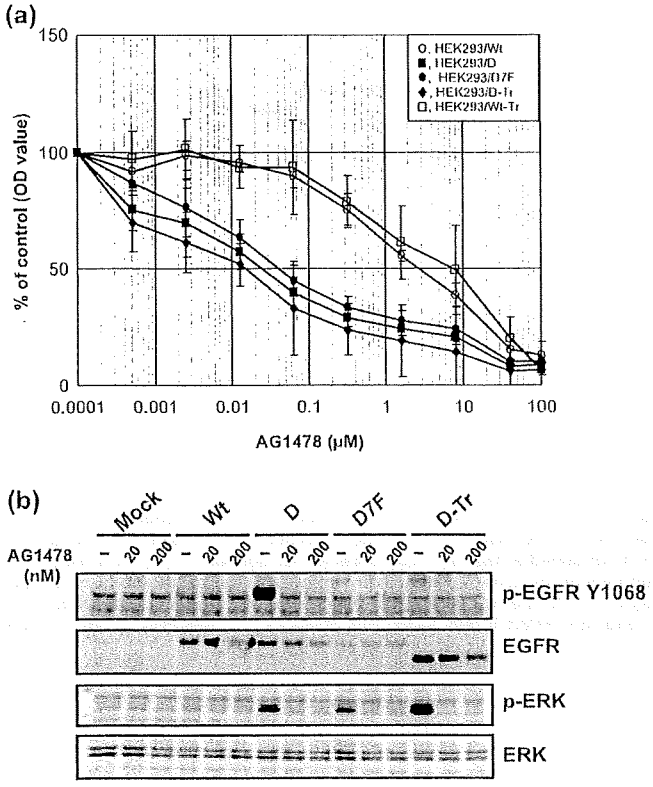

Fig. 3. Sensitivity of cell growth and downstream epidermal growth factor receptor (EGFR) signaling to AG1478 in the mutant EGFR transfectants. (a) The growth-inhibitory effect of AG1478 in HEK293/Wt, HEK293/Wt-Tr, HEK293/D, HEK293/D7F, and HEK293/D-Tr cells. The seeded cells were exposed to AG1478 for 72 h and the cellular proliferative activity was determined by MTT assay. (b) The HEK293/Wt, HEK293/D, HEK293/D7F, and HEK293/D-Tr cells were incubated in 1% serum starve medium for 12 h, followed by exposure to 20 or 200 nM AG1478 for 3 h at 37°C. The cell lysates were immunoblotted with anti-phospho-EGFR (p-EGFR Y1068), anti-EGFR (recognizing the extracellular domain), anti-phospho-ERK, or anti-ERK antibodies. Mock, HEK293/Mock; Wt, HEK293/Wt; Wt-Tr, HEK293/Wt-Tr; D, HEK293/D; D7F, HEK293/D7F; D-Tr, HEK293/D-Tr.

EGFR lacking C-terminal autophosphorylation sites with endogenous HER receptors contributes to the signal transduction. It is thus speculated that homodimerization of EGFR lacking C-terminal autophosphorylation sites transduces the signals to downstream molecules. Indeed, the results of the chemical crosslinking assay revealed clear homodimerized bands in the HEK293/Wt, HEK293/D, and HEK293/D7F cells (Fig. 5a). In the HEK293/D-Tr cells, homodimerized bands with lower molecular weights (indicated by the black arrow) were detected (Fig. 5a) and these dimers were not phosphorylated (Fig. 5b). Taken together, we speculate that EGFR lacking C-terminal autophosphorylation sites form homodimers.

Despite a lack of C-terminal autophosphorylation sites, transfected cells retain their capacity for EGFR-dependent Shc phosphorylation. Binding of adaptor proteins to the C-terminal region of EGFR is essential for EGFR signal transduction. It is widely recognized that tyrosines 1068 and 1086 are most important for Sos and Grb2 activation; EGFR-D7F and EGFR-D-Tr lack these tyrosine residues. Sos and Grb2 were coprecipitated with EGFR in the HEK293/Wt and HEK293/D cells, but not in the HEK293/D7F or HEK293/D-Tr cells (Fig. 6a). The bands were confirmed by reblotting of the membranes used for immunoblotting (data not shown). Another adaptor protein, Shc, also binds to the C-terminal region of EGFR, and phosphorylation of Shc activates the ERK pathway. An increase in phosphorylated p46 and p52 Shc was observed in the HEK293/D, HEK293/D7F, and HEK293/D-Tr cells compared with the HEK293/Mock and HEK/Wt cells (Fig. 6b). The phosphorylation of Shc observed in the HEK293/D, HEK293/D7F, and HEK293/D-Tr cells was completely inhibited by 20 nM AG1478 (Fig. 6c). These results suggest that EGFR lacking C-terminal autophosphorylation sites activates Shc in a C-terminal-independent manner, and that Shc-mediated signals may be involved in the hypersensitivity to EGFR TKI of HEK293 cells expressing EGFR lacking C-terminal autophosphorylation sites.

Discussion

In the present study, we investigated the relationship between phosphorylation of tyrosine residues in the C-terminal region of EGFR and cellular sensitivity to EGFR TKI. Increased phosphorylation of Shc and ERK was observed in HEK293/D7F and HEK293/D-Tr cells, which expressed EGFR lacking autophosphorylation sites in the C-terminal region. Previous reports have demonstrated

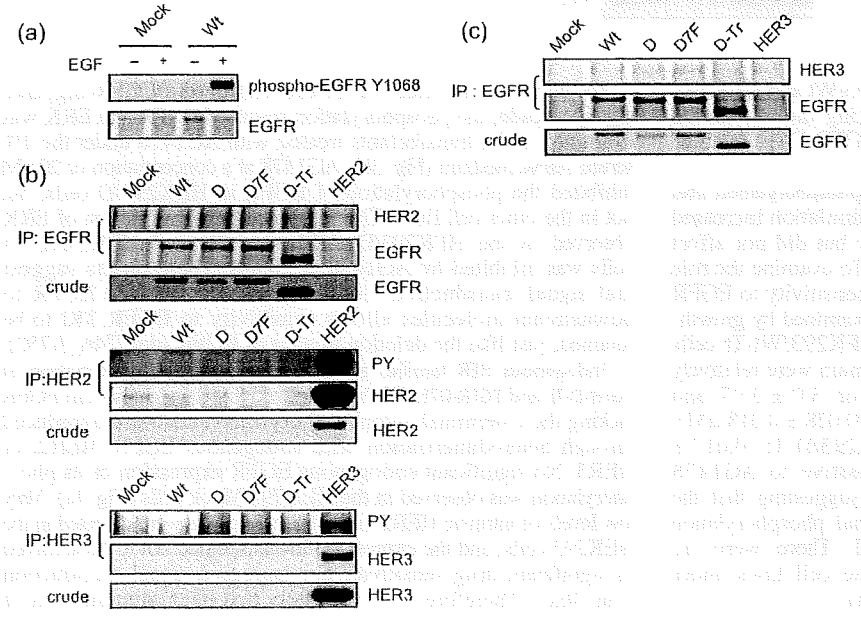

Fig. 4. Heterodimerization of mutant epidermal growth factor receptor (EGFR) with endogenous receptors of the HER family in mutant EGFR transfectants. Expression of endogenous EGFR and response to epidermal growth factor stimulation. HEK293/Mock, HEK293/Wt, HEK293/D, HEK293/D7F, and HEK293/D-Tr cells were incubated in 1% serum starve medium for 12 h followed by the addition of 10 ng/mL epidermal growth factor for 10 min at 37°C. (a) The whole-cell lysates of HEK293/Mock and HEK293/W+ cells containing equal amounts of protein were immunoblotted with anti-phospho-EGFR (p-EGFR Y1068) and anti-EGFR (recognized extracellular domain). (b,c) The lysates were immunoprecipitated with anti-EGFR, anti-HER2, or anti-HER3 antibodies, and immunoblotted with anti-EGFR, anti-HER2, anti-HER3, or anti-phosphotyrosine antibodies to detect the dimerization and phosphorylation of EGFR and endogenous HER2 or HER3. HER2, HER2-introduced HEK293 cells as a positive control; HER3, HER3-introduced HEK293 cells as a positive control.

doi: 10.1111/j.1349-7006.2008.01071.x

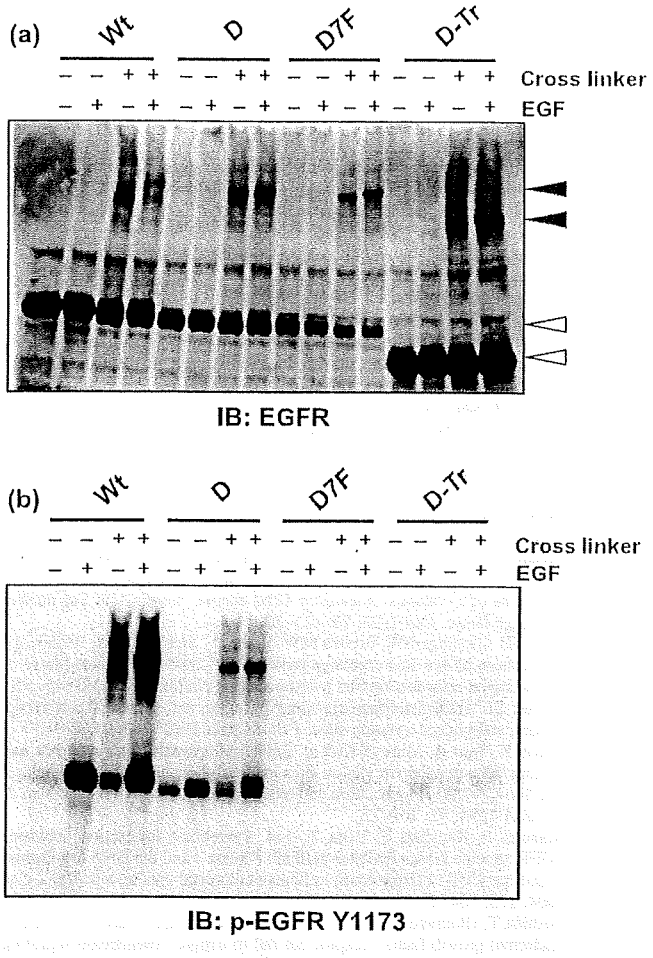

Fig. 5. The cells under 1% serum starved medium were allowed to react with 2 mM of the chemical crosslinking regent BS_3 before the crosslinking reaction was quenched. The cell lysates were immunoblotted with (a) anti-epidermal growth factor receptor (EGFR) (recognizing the extracellular domain) and (b) anti-phosphoEGFR (p-EGFR Y1173) antibodies to detect the dimerization and phosphorylation of wild-type and mutant EGFR. Black arrow, EGFR dimer; open arrow, EGFR monomer. Mock, HEK293/Mock; Wt, HEK293/Wt; D, HEK 293/D; D7F, HEK293/D7F; D-Tr, HEK293/D-Tr. EGF, epidermal growth factor.

that cells expressing EGFR lacking C-terminal autophospholylation sites retain EGF-induced mitogenic and transforming activity.[27,28] Our data and these previous reports suggest that there exist other EGFR signaling pathways besides those mediated by the C-terminal tyrosine residues. In addition, these signaling pathways are operative in the active EGFR mutant (delE746_A750) as well as wild-type EGFR.[28] The results of our growth-inhibition assay demonstrated the hypersensitivity of HEK293/D7F and HEK293/D-Tr cells to EGFR TKI, and phosphorylation of ERK and Shc in these cells was also inhibited. These results suggest that this EGFR signaling pathway contributes to tumor cell growth.

We demonstrated the hypersensitivity of the transfectants (HEK293/D7F and HEK293/D-Tr cells) to AG1478. We previously reported the hypersensitivity of transfectants carrying mutant EGFR to AG1478 as well as gefitinib, ZD6474, and erlotinib.[8,15,31] Therefore, it can be easily speculated that the HEK293/D7F and HEK293/D-Tr cells would also be hypersensitive to the clinically available EGFR TKI and AG1478.

Somatic EGFR mutation in lung cancer has been reported, and over 20 types of mutations have been reported.[10] The L858R point mutation in exon 21 of EGFR is a major point mutation (such as in delE746_A750) that contributes to EGFR TKI hypersensitivity.[32] Interestingly, we constructed cells that overexpressed EGFR-Wt-Tr and EGFR-D-Tr, and a mutant truncated form of EGFR similar to EGFR-Wt-Tr was previously found in patients with glioblastoma.[33] The mutant was truncated at amino acid 958 of EGFR and the frequency was relatively high in 7 of 48 patients. Therefore, it would be of interest to determine in future studies whether this C-terminal-truncated form of delE746_A750 EGFR, similar to EGFR-D-Tr, might be identifiable in human materials in the clinical setting.

We attempted to clarify the signaling pathway from the C-terminal region of EGFR. We observed the phosphorylation of ERK and Shc in HEK293/D7F and HEK293/D-Tr cells, and these phosphorylations were inhibited by exposure to AG1478. These phosphorylations were not observed in HEK293/Mock, HEK293/Wt, or HEK293/Wt-Tr cells. Our results suggest that the constitutively active mutant EGFR lacking C-terminal autophosphorylation sites is sufficient for activation of the downstream pathway. However, it remains unknown how signals are transduced from EGFR without a C-terminal region to Shc, as no direct binding of Grb2 or Shc with EGFR lacking the C-terminal region was detected in the HEK293/D7F and HEK293/D-Tr cells (Fig. 6a). We attempted to identify the mediator molecules binding to EGFR-D-Tr and EGFR-D7F by mass analysis of immunoprecipitates; however, no clear mediator molecules were identified. As a possible indirect mechanism, Sasaoka *et al.* postulated that ErbB2–Shc signals from EGFR lacking C-terminal autophosphorylation sites.[34] However, we consider this unlikely from the results of our experiments because no significant expression of Erb2 was detected in the HER293 cells.

The results of the crosslinking assay demonstrated that a complex of lower molecular weight was present in the HEK293/D-Tr cells compared with the HER293/Wt cells, indicating that truncated EGFR forms homodimers in the HEK293/D-Tr cells. Thus, it can be speculated that homodimerized truncated EGFR directly transduces signals downstream.

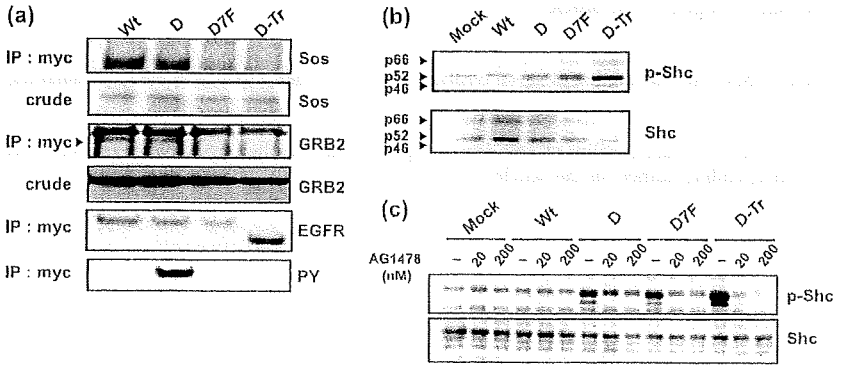

Fig. 6. Interaction between mutant epidermal growth factor receptor (EGFR) and adaptor proteins. The cells were cultured under normal conditions. (a) The lysates of HEK293/Wt, HEK293/D, HEK293/D7F, and HEK293/D-Tr cells were immunoprecipitated with anti-myc tag antibody; the precipitates were immunoblotted with anti-son of sevenless homolog (Sos) and anti-growth factor receptor-bound protein (Grb) 2 antibodies. (b) Whole-cell lysates containing equal amounts of protein were immunoblotted with anti-phospho-Src homology and collagen homology (Shc) and anti-Shc antibodies. (c) The cells incubated in 1% serum starve medium for 12 h were treated with 20 or 200 nM AG1478 for 3 h and then the lysates were immunoblotted with anti-phospho-Shc or anti-Shc antibodies. Mock, HEK293/Mock; Wt, HEK293/Wt; D, HEK293/D; D7F, HEK293/D7F; D-Tr, HEK293/D-Tr. PY, anti-phospho-tyrosine.

In conclusion, our results indicate that an as-yet-unknown signaling pathway of EGFR exists that is independent of the C-terminal region of EGFR, and these regions are not required for cellular sensitivity to EGFR TKI.

Acknowledgments

This work was supported by a research grant from the Third Term Comprehensive 10-Year Strategy for Cancer Control.

References

1 Gusterson B, Cowley G, McIlhinney J, Ozanne B, Fisher C, Reeves B. Evidence for increased epidermal growth factor receptors in human sarcomas. *Int J Cancer* 1985; **36**: 689–93.
2 Bargmann CI, Hung MC, Weinberg RA. The *neu* oncogene encodes an epidermal growth factor receptor-related protein. *Nature* 1986; **319**: 226–30.
3 Cowley GP, Smith JA, Gusterson BA. Increased EGF receptors on human squamous carcinoma cell lines. *Br J Cancer* 1986; **53**: 223–9.
4 Mendelsohn J, Baselga J. Epidermal growth factor receptor targeting in cancer. *Semin Oncol* 2006; **33**: 369–85.
5 Karamouzis MV, Grandis JR, Argiris A. Therapies directed against epidermal growth factor receptor in aerodigestive carcinomas. *JAMA* 2007; **298**: 70–82.
6 Rocha-Lima CM, Soares HP, Raez LE, Singal R. EGFR targeting of solid tumors. *Cancer Control* 2007; **14**: 295–304.
7 Paez JG, Janne PA, Lee JC *et al.* EGFR mutations in lung cancer: correlation with clinical response to gefitinib therapy. *Science* 2004; **304**: 1497–500.
8 Lynch TJ, Bell DW, Sordella R *et al.* Activating mutations in the epidermal growth factor receptor underlying responsiveness of non-small-cell lung cancer to gefitinib. *N Engl J Med* 2004; **350**: 2129–39.
9 Amann J, Kalyankrishna S, Massion PP *et al.* Aberrant epidermal growth factor receptor signaling and enhanced sensitivity to EGFR inhibitors in lung cancer. *Cancer Res* 2005; **65**: 226–35.
10 Mitsudomi T, Yatabe Y. Mutations of the epidermal growth factor receptor gene and related genes as determinants of epidermal growth factor receptor tyrosine kinase inhibitors sensitivity in lung cancer. *Cancer Sci* 2007; **98**: 1817–24.
11 Riely GJ, Pao W, Pham D *et al.* Clinical course of patients with non-small cell lung cancer and epidermal growth factor receptor exon 19 and exon 21 mutations treated with gefitinib or erlotinib. *Clin Cancer Res* 2006; **12**: 839–44.
12 Arao T, Fukumoto H, Takeda M, Tamura T, Saijo N, Nishio K. Small in-frame deletion in the epidermal growth factor receptor as a target for ZD6474. *Cancer Res* 2004; **64**: 9101–4.
13 Koizumi F, Shimoyama T, Taguchi F, Saijo N, Nishio K. Establishment of a human non-small cell lung cancer cell line resistant to gefitinib. *Int J Cancer* 2005; **116**: 36–44.
14 Naruse I, Ohmori T, Ao Y *et al.* Antitumor activity of the selective epidermal growth factor receptor-tyrosine kinase inhibitor (EGFR-TKI) Iressa (ZD1839) in an EGFR-expressing multidrug-resistant cell line *in vitro* and *in vivo*. *Int J Cancer* 2002; **98**: 310–15.
15 Sakai K, Arao T, Shimoyama T *et al.* Dimerization and the signal transduction pathway of a small in-frame deletion in the epidermal growth factor receptor. *FASEB J* 2006; **20**: 311–13.
16 Sakai K, Yokote H, Murakami-Murofushi K, Tamura T, Saijo N, Nishio K. In-frame deletion in the EGF receptor alters kinase inhibition by gefitinib. *Biochem J* 2006; **397**: 537–43.
17 Olayioye MA, Neve RM, Lane HA, Hynes NE. The ErbB signaling network: receptor heterodimerization in development and cancer. *EMBO J* 2000; **19**: 3159–67.
18 Yarden Y, Sliwkowski MX. Untangling the ErbB signalling network. *Nat Rev Mol Cell Biol* 2001; **2**: 127–37.
19 Batzer AG, Blaikie P, Nelson K, Schlessinger J, Margolis B. The phosphotyrosine interaction domain of Shc binds an LXNPXY motif on the epidermal growth factor receptor. *Mol Cell Biol* 1995; **15**: 4403–9.
20 Batzer AG, Rotin D, Urena JM, Skolnik EY, Schlessinger J. Hierarchy of binding sites for Grb2 and Shc on the epidermal growth factor receptor. *Mol Cell Biol* 1994; **14**: 5192–201.
21 Ono M, Hirata A, Kometani T *et al.* Sensitivity to gefitinib (Iressa, ZD1839) in non-small cell lung cancer cell lines correlates with dependence on the epidermal growth factor (EGF) receptor/extracellular signal-regulated kinase 1/2 and EGF receptor/Akt pathway for proliferation. *Mol Cancer Ther* 2004; **3**: 465–72.
22 Quesnelle KM, Boehm AL, Grandis JR. STAT-mediated EGFR signaling in cancer. *J Cell Biochem* 2007; **102**: 311–19.
23 Ravichandran KS, Lorenz U, Shoelson SE, Burakoff SJ. Interaction of Shc with Grb2 regulates association of Grb2 with mSOS. *Mol Cell Biol* 1995; **15**: 593–600.
24 Rubio I, Rennert K, Wittig U *et al.* Ras activation in response to phorbol ester proceeds independently of the EGFR via an unconventional nucleotide-exchange factor system in COS-7 cells. *Biochem J* 2006; **398**: 243–56.
25 Buday L, Downward J. Epidermal growth factor regulates p21ras through the formation of a complex of receptor, Grb2 adapter protein, and Sos nucleotide exchange factor. *Cell* 1993; **73**: 611–20.
26 Egan SE, Giddings BW, Brooks MW, Buday L, Sizeland AM, Weinberg RA. Association of Sos Ras exchange protein with Grb2 is implicated in tyrosine kinase signal transduction and transformation. *Nature* 1993; **363**: 45–51.
27 Decker SJ. Transmembrane signaling by epidermal growth factor receptors lacking autophosphorylation sites. *J Biol Chem* 1993; **268**: 9176–9.
28 Gotoh N, Tojo A, Muroya K *et al.* Epidermal growth factor-receptor mutant lacking the autophosphorylation sites induces phosphorylation of Shc protein and Shc-Grb2/ASH association and retains mitogenic activity. *Proc Natl Acad Sci USA* 1994; **91**: 167–71.
29 Koizumi F, Kanzawa F, Ueda Y *et al.* Synergistic interaction between the EGFR tyrosine kinase inhibitor gefitinib ('Iressa') and the DNA topoisomerase I inhibitor CPT-11 (irinotecan) in human colorectal cancer cells. *Int J Cancer* 2004; **108**: 464–72.
30 Yoshida T, Okamoto I, Okabe T *et al.* Matuzumab and cetuximab activate the epidermal growth factor receptor but fail to trigger downstream signaling by Akt or Erk. *Int J Cancer* 2008; **122**: 1530–8.
31 Arao T, Yanagihara K, Takigahira M *et al.* ZD6474 inhibits tumor growth and intraperitoneal dissemination in a highly metastatic orthotopic gastric cancer model. *Int J Cancer* 2006; **118**: 483–9.
32 Mitsudomi T, Kosaka T, Endoh H *et al.* Mutations of the epidermal growth factor receptor gene predict prolonged survival after gefitinib treatment in patients with non-small-cell lung cancer with postoperative recurrence. *J Clin Oncol* 2005; **23**: 2513–20.
33 Frederick L, Wang XY, Eley G, James CD. Diversity and frequency of epidermal growth factor receptor mutations in human glioblastomas. *Cancer Res* 2000; **60**: 1383–7.
34 Sasaoka T, Langlois WJ, Bai F *et al.* Involvement of ErbB2 in the signaling pathway leading to cell cycle progression from a truncated epidermal growth factor receptor lacking the C-terminal autophosphorylation sites. *J Biol Chem* 1996; **271**: 8338–44.

Supporting Information

Additional Supporting Information may be found in the online version of this article:

Table S1. Primer set for epidermal growth factor receptor cDNA with substitution of seven tyrosine residues to phenylalanine in the C-terminal region

Please note: Wiley-Blackwell are not responsible for the content or functionality of any supporting materials supplied by the authors. Any queries (other than missing material) should be directed to the corresponding author for the article.

doi: 10.1111/j.1349-7006.2008.01071.x

the FEBS Journal

Mitogen-activated protein kinase phosphatase-1 modulated JNK activation is critical for apoptosis induced by inhibitor of epidermal growth factor receptor-tyrosine kinase

Kenji Takeuchi[1], Tomohiro Shin-ya[1], Kazuto Nishio[2] and Fumiaki Ito[1]

1 Department of Biochemistry, Faculty of Pharmaceutical Sciences, Setsunan University, Osaka, Japan
2 Department of Genome Biology, Kinki University School of Medicine, Osaka, Japan

Keywords
AG1478; c-Jun N-terminal kinase; epidermal growth factor receptor; mitogen-activated protein kinase phosphatase-1; non-small-cell lung cancer

Correspondence
K. Takeuchi, Department of Biochemistry, Faculty of Pharmaceutical Sciences, Setsunan University, Hirakata, Osaka 573-0101, Japan
Fax: +81 72 866 3117
Tel: +81 72 866 3118
E-mail: takeuchi@pharm.setsunan.ac.jp

(Received 29 August 2008, revised 6 December 2008, accepted 16 December 2008)

doi:10.1111/j.1742-4658.2008.06861.x

Alterations resulting in enhanced epidermal growth factor receptor (EGFR) expression or function have been documented in a variety of tumors. Therefore, EGFR-tyrosine kinase is a promising therapeutic target. Although *in vitro* and *in vivo* studies have shown the anti-tumor activity of EGFR-tyrosine kinase inhibitors against various tumor types, little is known about the mechanism by which such inhibitors effect their anti-tumor action. AG1478 is known to selectively inhibit EGFR-tyrosine kinase. In this study, we showed that AG1478 caused apoptosis and apoptosis-related reactions such as the activation of caspase 3 in human non-small cell lung cancer cell line PC-9. To investigate the signaling route by which AG1478 induced apoptosis, we examined the activation of c-Jun N-terminal kinase (JNK) and mitogen-activated protein kinase p38 in AG1478-treated PC-9 cells. JNK, but not p38, was significantly activated by AG1478 as determined by both immunoblot analysis for levels of phosphorylated JNK and an *in vitro* activity assay. Various types of stimuli activated JNK through phosphorylation by the dual-specificity JNK kinases, but the dual-specificity JNK kinases MKK4 and MKK7 were not activated by AG1478 treatment. However, JNK phosphatase, i.e. mitogen-activated protein kinase phosphatase-1 (MKP-1), was constitutively expressed in the PC-9 cells, and its expression level was reduced by AG1478. The inhibition of JNK activation by ectopic expression of MKP-1 or a dominant-negative form of JNK strongly suppressed AG1478-induced apoptosis. These results reveal that JNK, which is activated through the decrease in the MKP-1 level, is critical for EGFR-tyrosine kinase inhibitor-induced apoptosis.

Epidermal growth factor receptor (EGFR), a member of the ErbB family, is important in the regulation of growth, differentiation and survival of various cell types. Ligand binding to EGFR results in receptor dimerization, activation of its tyrosine kinase and phosphorylation of its C-terminal tyrosine residues. The tyrosine-phosphorylated motifs of EGFR recruit various adaptors or signaling molecules [1,2]. EGFR is able to activate a variety of signaling pathways through its association with these molecules. The mitogen-activated protein kinase (MAPK) pathway leading to phosphorylation of extracellular signal-regulated

Abbreviations
EGFR, epidermal growth factor receptor; ERK, extracellular signal-regulated kinase; JNK, c-Jun N-terminal kinase; MAPK, mitogen-activated protein kinase; MKP-1, mitogen-activated protein kinase phosphatase-1; NSCLC, non-small-cell lung cancer; PI, propidium iodide; PtdIns3-K, phosphatidylinositol 3-kinase; SAPK, stress-activated MAPK.

kinase (ERK) 1/2 plays an essential role in EGF-induced cell growth; and the phosphatidylinositol 3-kinase (PtdIns3K) pathway is also important for cell growth and cell survival. One way by which PtdIns3K signals cells to survive is by activating protein kinase PDK1 which in turn phosphorylates Akt.

EGFR gene mutations or EGFR gene amplification is detected in various types of malignancy [1,2]; therefore, EGFR-tyrosine kinase is a promising therapeutic target. Orally active small molecules against EGFR (e.g. gefitinib and erlotinib) show evident anti-tumor effects in patients with various cancers, particularly non-small cell lung cancer (NSCLC) [3–5]. Beneficial responsiveness to EGFR-targeting chemicals in NSCLC patients is closely associated with EGFR mutations in the kinase domain [6–8].

The induction of apoptosis has been considered as a major mechanism for gefitinib-mediated anti-cancer effects [9,10]. Lung cancer cells harboring mutant EGFRs become dependent on them for their survival and, consequently, undergo apoptosis following inhibition of EGFR tyrosine kinase by gefitinib. Gefitinib has been shown to inhibit cell survival and growth signaling pathways such as the Ras-MAPK pathway and PtdIns3K/Akt pathway, as a consequence of inactivation of EGFR [10–13]. The PtdIns3K/Akt pathway is downregulated in response to gefitinib only in NSCLC cell lines that are growth-inhibited by gefitinib [14]. So, it is thought that the PtdIns3K/Akt pathway plays a critical role in the gefitinib-induced anti-tumor action. Furthermore, some reports have demonstrated that blockage of the EGFR activity with gefitinib is able to cause suppression of a downstream signaling pathway through Ras-MAPK and/or PtdIns3K/Akt, and induce apoptosis through activation of the pro-apoptotic Bcl-2 family protein Bad or Bax [9,15].

In mammals, three major groups of MAPK have been identified [16–18]. The c-Jun N-terminal kinase (JNK), also known as stress-activated MAPK (SAPK), represents a group of MAPKs that are activated by treatment of cells with cytokines or by exposure of cells to a variety of stresses [19–21]. JNK activity has been implicated in both apoptosis and survival signaling and is tightly controlled by both protein kinases and protein phosphatases [22–24]. Various types of stimuli activate JNK through phosphorylation by the dual-specificity kinase MKK4 or MKK7 [18,25]. By contrast, any types of stimuli can inactivate JNK through induction of the expression of JNK phosphatases, which include dual-specificity (threonine/tyrosine) phosphatases [26–28].

PC-9 cells are gefitinib-sensitive human NSCLC cell lines with a mutation (delE746-A750) in their EGFR, which allows the receptor to be autophosphorylated independent of EGF. In this study, we investigated the signaling route by which the EGFR tyrosine kinase inhibitor AG1478 induces apoptosis in PC-9 cells. There is a general agreement on the hypothesis that the inhibition of ERK1/2 MAPK and/or PtdIns3K/Akt growth/survival signaling cascades leads to apoptosis of cancer cells. However, there are no studies addressing the role of JNK in apoptosis induced by EGFR tyrosine kinase inhibitors. Here, we demonstrate that JNK-phosphatase MKP-1 expression is controlled by a signal downstream of EGFR and that if this signal is abolished by an inhibitor of EGFR tyrosine kinase, the decreased MKP-1 activity can result in JNK activation, leading to the induction of apoptosis.

Results

We first examined the effect of AG1478 on the viability of human NSCLC cell line PC-9. Treatment of the cells with AG1478 markedly suppressed the cell viability, as determined by the results of a colorimetric assay (Fig. 1A). Photographic observation of AG1478-treated PC-9 cells revealed that AG1478 decreased the percentage of adherent cells in a time-dependent manner (Fig. 1B). When AG1478-treated PC-9 cells were stained with Hoechst–propidium iodide (PI), cells with condensed chromatin and fragmented nuclei, which are characteristic of the nuclear changes in apoptotic cells, were seen in both adherent and non-adherent cell populations (data not shown). To confirm whether this AG1478-induced cell death resulted from apoptosis, we examined caspase 3 activity after exposing the cells to 500 nM AG1478. As shown in Fig. 1C, caspase 3 activity was increased in a time-dependent manner. It thus appears that AG1478 reduced the survival rate of PC-9 cells by activating the apoptotic pathway.

It is important to know how AG1478 affected the survival rate of PC-9 cells. Many studies have shown that enhanced JNK activity may be required for initiation of stress-induced apoptosis [29,30]. To examine whether JNK might be activated by AG1478, we treated PC-9 cells with AG1478 for various periods (Fig. 2A). Activation of JNK was measured by performing an immune complex kinase assay using bacterially expressed GST–c-Jun as a substrate. Phosphorylation of c-Jun appeared 1 h after AG1478 addition, with a maximum level at 24 h. We next determined the phosphorylation of JNK in the presence of AG1478. PC-9 cells were incubated with AG1478 for several periods, and cell lysates were prepared from these cells to determine the phosphorylation of JNK by immunoblotting (Fig. 2B). AG1478

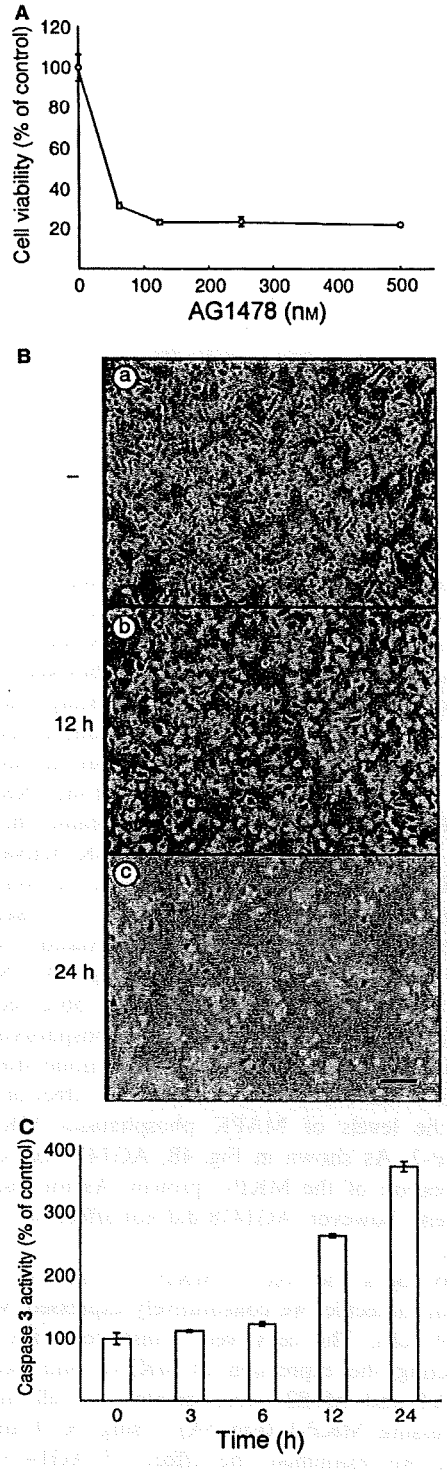

Fig. 1. Induction of apoptosis by AG1478. (A) PC-9 cells were seeded into a 96-well microplate, and treated with AG1478 at various concentrations for 48 h. The viability of cells was determined by conducting WST-8 assays. The value of untreated cells was considered as 100% viability. The data presented are the mean ± SD ($n = 6$). (B) PC-9 cells were seeded at a density 3×10^5 cells per 60 mm dish and then treated with 500 nM AG1478. The phase-contrast photomicrographs were taken 0 (a), 12 (b) or 24 h (c) after incubation with AG1478. Scale bar, 100 μm. (C) PC-9 cells were treated with 500 nM AG1478. Lysates were prepared at the indicated time points after the AG1478 addition and analyzed for caspase **3** activity by using a fluorometric substrate-based assay. Each point is the mean of triplicate samples, and the bar represents the standard deviation. Similar results were obtained from three separate experiments.

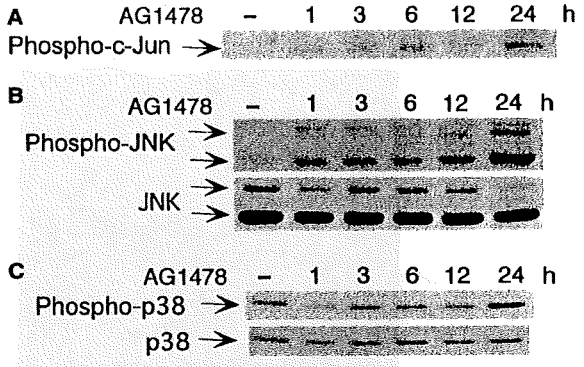

Fig. 2. JNK activation by AG1478. PC-9 cells were treated with 500 nM AG1478 and lysed on ice at the indicated time points. (A) JNK–c-Jun complexes were collected by glutathione *S*-transferase–c-Jun agarose beads and then assayed *in vitro* for kinase activity by using c-Jun as a substrate. The phospho-c-Jun product was detected by immunoblotting. (B) The cell lysates were normalized for protein content and analyzed for phospho-JNK content (upper), as well as for JNK content (lower). (C) The cell lysates were analyzed for phospho-p38 content (upper panel), as well as for p38 (lower). Similar results were obtained from three separate experiments.

intensively stimulated phosphorylation of JNK on its threonine 183 and tyrosine 185, and their phosphorylation levels continued to increase for at least 24 h. However, the activation of p38, another MAP kinase sub-family member, was not evident up to 12 h after AG1478 treatment; although an increase in the phosphorylation of p38 was detected at 24 h (Fig. 2C). Phosphorylation of ERK1/2, prototypical MAPK, was decreased by the treatment with AG1478 at the same time as activation of JNK (data not shown).

Neither SB203580 nor PD98059, inhibitors of p38 and ERK1/2, respectively, affected AG1478-induced apoptosis in PC-9 cells (data not shown), suggesting that neither p38 nor ERK1/2 mainly transmit the apoptotic signal of AG1478 in the PC-9 cells. If JNK plays an important role in AG1478-induced apoptosis,

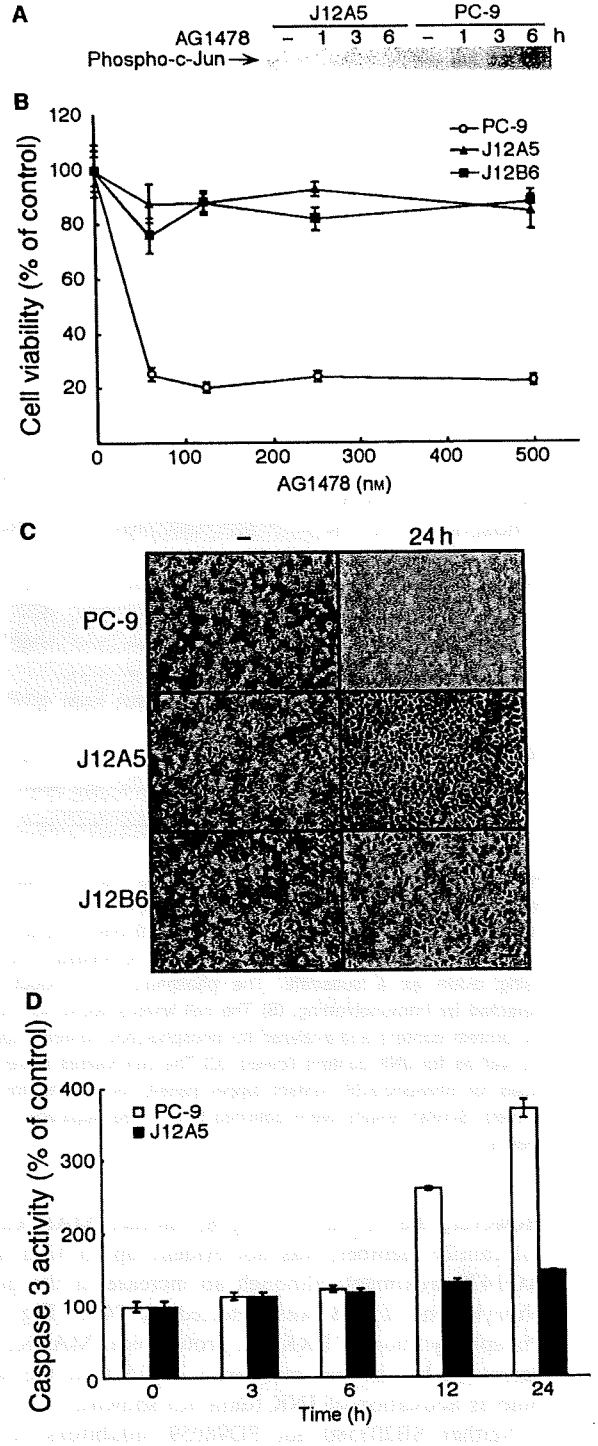

Fig. 3. Expression of dominant-negative JNK prevents AG1478-induced apoptosis. (A) Subconfluent PC-9 and J12A5 cells were incubated with 500 nM AG1478 for the indicated times. JNK activity was determined as described in Experimental Procedures. (B) PC-9, J12A5 and J12B6 cells were incubated with the indicated concentrations of AG1478 for 48 h. The viability of cells was determined by conducting WST-8 assays. The reading obtained for untreated cells was considered as 100% viability. The data presented are the mean ± SD (n = 6). (C) Phase-contrast photomicrographs were taken 24 h after incubation with 500 nM AG1478. Scale bar, 100 μm. (D) PC-9 and J12A5 cells were treated with 500 nM AG1478. Lysates were prepared at the indicated time points after the AG1478 addition and analyzed for caspase **3** activity by using a fluorometric substrate-based assay. Each point is the mean of the triplicate samples, and the bar represents the standard deviation. Similar results were obtained from three separate experiments.

inactivation of JNK should suppress this AG1478-induced apoptosis. To test this scenario, we stably transfected PC-9 cells with a mammalian expression vector encoding a dominant-negative form of JNK, and isolated two clones, J12A5 and J12B6. The results of a JNK kinase assay confirmed that J12A5 cells had no detectable activity (Fig. 3A). A colorimetric assay for cell viability, microscopic observation of cells, and an assay for caspase **3** activity revealed that this dominant-negative kinase efficiently blocked AG1478-induced apoptosis (Fig. 3B–D), indicating that activation of JNK mediated the AG1478-induced apoptosis.

A multitude of stimuli including osmotic stress activate JNK through phosphorylation of the JNK kinases MKK4 and MKK7 [18,31]. To examine the mechanism by which AG1478 induced JNK activation, we incubated PC-9 cells in the presence of AG1478 for several periods, and then prepared cell lysates from these cells to determine the phosphorylation of MKK4 and MKK7 by immunoblotting (Fig. 4A). No phosphorylated MKK4 or MKK7 was observed in the presence of AG1478, although phosphorylation of both JNK kinases in response to osmotic stress could be detected. Next, we determined the effect of AG1478 on the levels of MAPK phosphatases MKP-1 and MKP-2. As shown in Fig. 4B, AG1478 decreased the expression of the MKP-1 protein. As for the MKP-2 protein, however, AG1478 did not affect its expression level.

To check the role of MKP-1 as an anti-apoptotic signal molecule, we constitutively expressed MKP-1 in PC-9 cells. The cells were transfected with a vector directing the expression of MKP-1; and two clones, M1A4 and M1B2, were isolated as cell lines overexpressing MKP-1 (Fig. 5A). Using PC-9 and M1A4 cells, we examined the effect of AG1478 on the amounts of dually phosphorylated JNK (Fig. 5B). In PC-9 cells, AG1478 treatment decreased the expression of the MKP-1 protein and concomitantly stimulated the phosphorylation of JNK. However, the expression

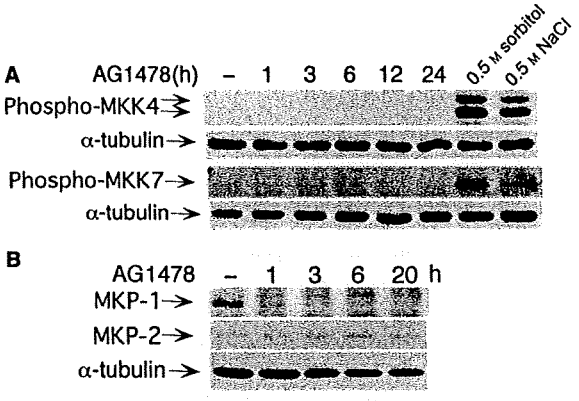

Fig. 4. Effect of AG1478 on phosphorylation of MKK4 and MKK7, and expression of MKP-1 and MKP-2. A, PC-9 cells were treated with 500 nM AG1478 for the indicated periods, and cellular lysates were analyzed by SDS/PAGE and immunoblotting with anti-[phospho SEK1/MKK4 (Ser254/Thr261)] Ig and anti-[phospho MKK7 (Ser271/Thr275)] Ig, respectively (upper). α-Tubulin levels were examined as a control for equal loading (lower). As a control for MKK4 and MKK7 activation, parallel cultures were treated with 0.5 M sorbitol for 30 min or with 0.5 M sodium chloride for 15 min. (B) The cellular lysates were prepared at the indicated time points after AG1478 treatment. Total protein (40 μg) was subjected to immunoblotting, and the membranes were hybridized with antibodies against MKP-1 (upper) or MKP-2 (middle). The equal loading of the samples was checked by using an antibody against α-tubulin (lower). The experiments corresponding to (A) and (B) were repeated three times with similar results.

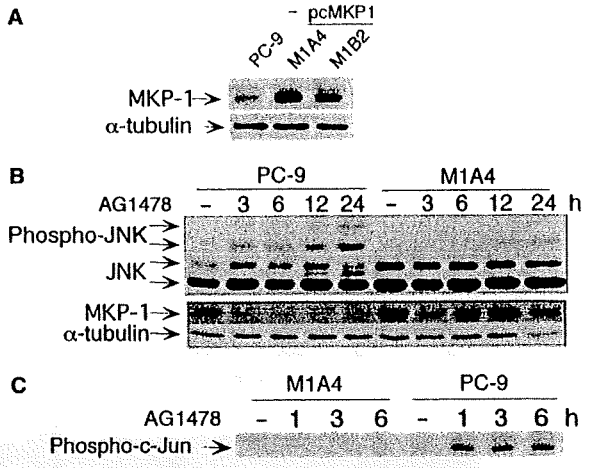

Fig. 5. Expression of MKP-1 prevents JNK activation. (A) Cellular lysates were prepared from parent PC-9 cells and pcMKP1- transfected PC-9 cells (M1A4 and M1B2). The lysates were analyzed by SDS/PAGE and immunoblotting with specific antibody against MKP-1 (upper) or α-tubulin (lower). (B) Subconfluent PC-9 and M1A4 cells were incubated with 500 nM AG1478 for the indicated times. The cells were then harvested, and equal aliquots of protein extracts (40 μg per lane) were analyzed for phospho-JNK (upper) and MKP-1 (lower) by immunoblotting. Each membrane was reprobed with JNK (upper) or an α-tubulin antibody (lower). Similar results were obtained from three separate experiments. (C) Cell lysates were prepared from PC-9 and M1A4 cells at the indicated time points after treatment with 500 nM AG1478. JNK activity was determined as described in Experimental procedures. The experiments were repeated three times with similar results.

level of MKP-1 in M1A4 cells remained high, in contrast to that in PC-9 cells; although MKP-1 expression was lowered once at 3 h after AG1478 treatment. JNK phosphorylation was extremely low in M1A4 cells. The expression patterns of MKP-1 and phospho-JNK seen in M1A4 were also observed in M1B2 cells (data not shown). The results of the JNK kinase assay indicated that JNK was not activated in M1A4 cells, where the MKP-1 expression level remained high even after exposure to AG1478 (Fig. 5C).

We next tested whether the expression level of MKP-1 correlated with sensitivity to AG1478. As shown in Fig. 6A,B, overexpression of MKP-1 resulted in resistance to AG1478. We also examined whether AG1478 could activate the effector caspase 3 in M1A4 cells (Fig. 6C). In PC-9 cells, activation of caspase 3 was observed with a maximal increase (480%) at 24 h after AG1478 treatment; however, in M1A4 cells, only a slight increase in caspase 3 enzyme activity (28% and 39% at 12 and 24 h, respectively) was detected. These results show that the MKP-1 expression level correlated with the susceptibility to AG1478-induced apoptosis.

Discussion

Gefitinib, an EGFR-tyrosine kinase inhibitor, has been reported to inhibit cell survival and proliferation signaling pathways such as MAPK and PtdIns3K/Akt pathways [10–13]. Furthermore, some reports have shown that gefitinib reduces Akt activity only in NSCLC cell lines, in which it inhibits growth [14,32]. The ErbB family of receptor tyrosine kinases includes four members, namely, the EGFR (ErbB1), ErbB2, ErbB3 and ErbB4. Among these members, ErbB3 effectively couples to the PtdIns3K/Akt pathway. Therefore, it is likely that ErbB3 serves to couple EGFR to the PtdIns3K/Akt pathway and that ErbB3 expression serves as an effective predictor of sensitivity to gefitinib in NSCLC cell lines [14]. In this study, we used PC-9 cells, which are gefitinib-sensitive human NSCLC cells with a mutation (delE746-A750) in their EGFR. In these PC-9 cells, autophosphorylation of EGFR took place independent of EGF, and it was suppressed by AG1478. Because AG1478 inhibited the phosphorylation of multiple down-stream targets including ERK1/2 in the PC-9 cells, but its effect on Akt phosphorylation was not so

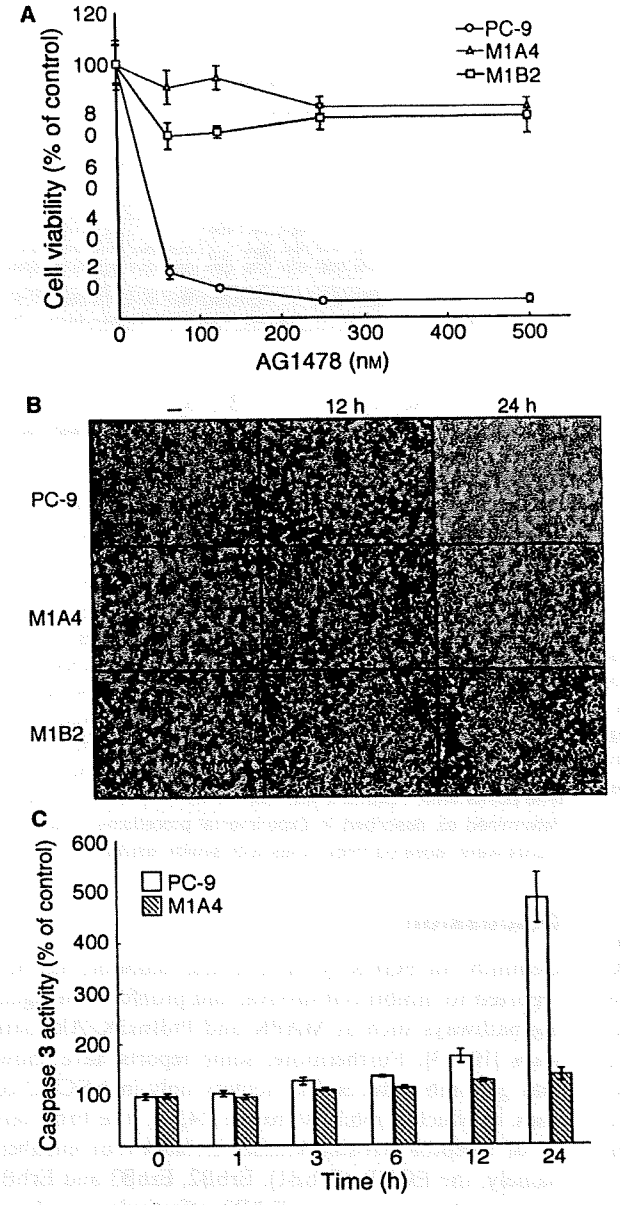

Fig. 6. Expression of MKP-1 prevents AG1478-induced apoptosis. A, PC-9, M1A4, and M1B2 cells were incubated with the indicated concentrations of AG1478 for 48 h. The viability of cells was determined by conducting WST-8 assays. The reading obtained for untreated cells was considered as 100% viability. The data presented are the mean ± SD (n = 6). (B) Phase-contrast photomicrographs were taken 12 and 24 h after incubation with 500 nM AG1478. Scale bar, 100 μm. (C) PC-9 and M1A4 cells were treated with 500 nM AG1478. Lysates were prepared at the indicated time points after the AG1478 addition and analyzed for caspase **3** activity by using a fluorometric substrate-based assay. Each point is the mean of the triplicate samples, and the bar represents the standard deviation. Similar results were obtained from three separate experiments.

significant (K. Takeuchi & F. Ito, unpublished data), intracellular signaling pathways other than PtdIns3K/Akt could be responsible for the AG1478-induced apoptosis in PC-9 cells.

Stress stimuli that induce apoptosis, including UV- and γ-irradiation, heat shock, protein synthesis inhibitors, DNA-damaging agents and the proinflammatory cytokines, are potent activators of JNK. Several anti-neoplastic agents such as cisplatin, etoposide, camptothecin and taxol, which are also strong inducers of apoptosis, also activate the JNK pathway [33]. In this study, we found that AG1478 induced the activation of JNK in PC-9 cells. Furthermore, a dominant-negative form of JNK efficiently blocked AG1478-induced apoptosis. It thus appears that EGFR-tyrosine kinase inhibitors induce apoptosis in PC-9 cells via activation of JNK.

ERK1 and ERK2, also known as p44 and p42 MAPK, respectively, represent the prototypical MAPK in mammalian cells. ERK MAP kinase catalytic activation was observed in PC-9 cells, and it was inhibited by AG1478. Increased phosphorylation of the other MAPK family member, p38, was also observed at 24 h after AG1478 treatment; but it was not observed at 12 h when apoptosis could be detected (Figs 1A and 2C). Our experiment indicated that neither SB203580 nor PD98059, inhibitors of p38 and ERK1/2, respectively, affected AG1478-induced apoptosis in PC-9 cells. Taken together, our data indicate that JNK, but not other MAPK family members such as p38 and ERK1/2, mainly transmits the apoptotic signal of AG1478 in the PC-9 cells.

JNK signaling can regulate apoptosis both positively and negatively, depending on the cell type, cellular context and the nature and dose of treatment [22,23]. Strong and sustained JNK activation is predominantly associated with induction or enhancement of apoptosis, whereas transient JNK activation can result in cell survival [23,24]. AG1478 induced strong and sustained JNK activation in PC-9 cells (Fig. 2A,B). This finding strengthens the possibility that JNK is a mediator of the apoptotic action of AG1478.

JNK activity in cells is tightly controlled by both protein kinases such as MKK4 or MKK7 and protein phosphatases such as MKPs. MKP-1, the first member of the MKP family to be identified as an ERK-specific phosphatase, is also able to inactivate JNK and p38 [34–38]. MKP-1 is an immediate-early gene whose expression is regulated by mitogenic, inflammatory and DNA-damaging stimuli [39–41]. In this study, we observed no activation of MKK4 or MKK7 in AG1478-treated PC-9 cells (Fig. 4A). However, the expression level of MKP-1, but not that of MKP-2,

was significantly decreased by the AG1478 treatment (Fig. 4B), indicating that JNK activity in the PC-9 cells may be regulated by MKP-1. Another member of the dual-phosphatase family of proteins, MKP-2 shows a 60% sequence homology to MKP-1, and also similar substrate specificity [42]. However, the expression level of MKP-2 was not affected by AG1478 treatment, indicating that the expression of MKP-1, but not that of MKP-2, is controlled by signals via EGFRs.

Brondello *et al.* reported that activation of the ERK cascade is sufficient to promote the expression of MKP-1 and MKP-2 [43]. It has also been suggested that MKP-1 expression is regulated by ERK-dependent and -independent signals [44]. Because the ERK inhibitor PD98059 did not affect MKP-1 expression or activation of JNK in PC-9 cells (K. Takeuchi & F. Ito, unpublished data), MPK-1 expression in PC-9 cells may be controlled in an ERK-independent manner. Recently, Ryser *et al.* reported that MKP-1 transcription is regulated in the transcriptional elongation step: under basal conditions, a strong block to elongation in the first exon regulates MKP-1 gene transcription [45]. Thus, EGFR-mediated signals may overcome this block to stimulate MKP-1 gene transcription in PC-9 cells. Another possible mechanism responsible for EGFR-mediated enhancement of MKP-1 expression is that MKP-1 degradation via the ubiquitin–proteasome pathway is suppressed by EGFR activation. In fact, some research groups have reported that the expression level of MKP-1 is controlled via the ubiquitin–proteasome pathway [46,47]. Our preliminary experiment also indicated that AG1478-induced MKP-1 degradation was suppressed in the presence of proteasome inhibitors such as MG-132 and ALLN (K. Takeuchi & F. Ito, unpublished data).

Gene disruption studies demonstrate that JNK is required for the release of mitochondrial proapoptotic molecules (including cytochrome *c*) and apoptosis in response to UV radiation [48]. Bax and Bak (members of the proapoptotic group of multidomain Bcl-2-related proteins) are essential for the JNK-stimulated release of cytochrome *c* and apoptosis [49]. Other studies have shown that 14-3-3 proteins are direct targets of JNK and that phosphorylation of 14-3-3 proteins by JNK results in dissociation of Bax from 14-3-3 proteins, leading to apoptosis [50]. Because translocation of Bax to mitochondria was observed in AG1478-treated PC-9 cells (K. Takeuchi & F. Ito, unpublished data), AG1478 may exert its apoptotic actions, at least in part, by promoting the translocation of Bax to mitochondria.

Some reports have shown that the activation of the Fas/FasL system may be one of the mechanisms responsible for drug-induced apoptosis in a variety of cancer cells of different histotype [51]. Chang *et al.* recently reported that an increase in Fas protein expression might be the molecular mechanism by which gefitinib induces apoptosis in lung cancer cell lines [52]. Furthermore, it has been reported that c-Jun-dependent FasL expression plays a critical role in the induction of apoptosis by genotoxic agents [53]. To understand the causal relationship between JNK activation and AG1478-induced apoptosis, we need to study whether AG1478 induces the expression of Fas or FasL in PC-9 cells.

Overexpression of MKP-1 inhibited the AG1478-induced JNK activation and also AG1478-induced apoptosis. These results indicate that there is a link between the decreased MKP-1 activity and AG1478-induced apoptosis: MKP-1 expression is controlled by signals downstream of EGFR, and it is downregulated in the presence of an inhibitor of EGFR tyrosine kinase. This downregulation could be followed by JNK activation, triggering the apoptosis pathway.

Understanding the molecular basis of responsiveness to gefitinib is important to identify patients who will have a positive response to this drug. The EGFR gene in tumors from patients with gefitinib-responsive lung cancer was recently examined for mutations, and clustering of mutations was detected in the part of the gene encoding the ATP-binding pocket. Screening for such mutations may identify patients who will have a positive response to the drug. However, this study showed that NSCLC cell line PC-9 was dependent on the MKP-1/JNK pathway for its growth and survival. Thus, sensitivity to gefitinib may be predicted from the detailed analysis of the MKP-1/JNK pathway as described in this study. Although the MKP-1 level in normal cells is low, an increased level of MKP-1 has been found in human ovarian, breast, and prostate cancer [54–56]. Our results suggest that MKP-1 may be a candidate drug target in order to optimize gefitinib-based therapeutic protocols.

Experimental procedures

Materials

EGF (ultra-pure) from mouse submaxillary glands was purchased from Toyobo Co., Ltd (Osaka, Japan). Fetal calf serum came from Gibco (Grand Island, NY, USA). Phenylmethanesulfonyl fluoride, pepstatin A, aprotinin and leupeptin were obtained from Sigma (St Louis, MO, USA). RPMI-1640 medium was from Nissui Pharmaceutical Co., Ltd (Tokyo, Japan). Antibodies used and their sources were: ERK1/2 (pT202/pY204) phospho-specific antibody (clone 20A), JNK(pT183/pY185) phospho-specific antibody